Chapter

Transceiver Design for Wireless Power Transfer for Multiuser MIMO Communication Systems

Anming Dong and Haixia Zhang

Abstract

This chapter describes transceiver design methods for simultaneous wireless power transmission (WPT) and information transmission in two typical multiuser MIMO networks, that is, the MIMO broadcasting channel (BC) and interference channel (IC) networks. The design problems are formulated to minimize the transmit power consumption at the transmitter(s) while satisfying the quality of service (QoS) requirements of both the information decoding (ID) and WPT of all users. The mean-square error (MSE) and the signal-to-interference-noise ratio (SINR) criteria are adopted to characterize the ID performance of the BC network and the IC network, respectively. The designs are cast as nonconvex optimization problems due to the coupling of multiple variables with respect to transmit precoders, ID receivers, and power splitting factors, which are difficult to solve directly. The feasibility conditions of these deign problems are discussed, and effective solving algorithms are developed through alternative optimization (AO) framework and semidefinite programming relaxation (SDR) techniques. Low-complexity algorithms are also developed to alleviate the computation burden in solving the semidefinite programming (SDP) problems. Finally, simulation results validating those proposed algorithms are included.

Keywords: wireless power transfer (WPT), energy harvesting, multiuser MIMO, transceiver design, alternating optimization, semidefinite programming relaxation (SDR)

1. Introduction

Wireless power transfer (WPT) through radio frequency (RF) signals has been redeemed as one of the promising techniques to provide perpetual and cost-effective power supplies for mobile devices [1–4]. Compared with traditional energy harvesting (EH) methods depending on external sources, such as solar power and wind energy, the RF WPT is able to power the wireless devices at any time. Moreover, since RF signals carry energy as well as information, wireless devices can be charged while communicating. These merits of WPT bring great convenience and provide quality of service (QoS) guarantee for wireless devices.

On the other hand, multiple-input, multiple-output (MIMO) techniques are widely used in many wireless communication systems such as WiFi and the fifth generation mobile (5G) systems, due to their potential in providing increased link capacity and spectral efficiency combined with improved link reliability. Moreover, the evolution of MIMO techniques to the massive MIMO systems, where tens or hundreds of antennas are equipped at transmitters or/and receivers, accompanied by shrinking coverage of base stations (BSs) in the future wireless systems, makes it possible to transmit wireless power with higher efficiency. It is envisaged that the power line connected to the mobile devices would be eliminated completely in future wireless communications by combing WPT with MIMO wireless information transmission (WIT) system [5–9].

Transceiver design plays a very important role in achieving this vision. The objective of the transceiver design is to improve the energy and spectral efficiency of the transmitter by optimizing the beam patterns of the transmitting antennas and the filters at the information decoding (ID) receivers. However, it is not a trivial task to design transceivers for multiuser MIMO systems operating in simultaneous wireless information and power transfer (SWIPT) mode due to the presence of inter-user interference. The interference makes the whole design complicated since it is harmful to WIT but beneficial to WPT, and it is very challenging to balance the role of interference in ID and EH. And what makes things worse is that the interference and the PS factors are coupled together, which makes the joint transceiver design and power splitting (JTPS) problems nonconvex. These problems are NP-hard in general, so effective algorithms should be found to get feasible solutions.

In this chapter, we will discuss transceiver design methods for SWIPT in two typical multi-user MIMO scenarios, that is, the broadcasting channel (BC) network and interference channel (IC) network. We focus on the QoS-constrained problems that are formulated as minimizing the transmit power consumption subject to both the minimum ID and EH requirements. The mean-square error (MSE) and the signal-to-interference-noise ratio (SINR) criteria are adopted to characterize the ID performance of the two kinds of network, respectively. The formulated optimization problems are nonconvex with respect to the optimization variables, that is, the parameters of transmit precoders, ID receivers, and PS factors. In order to develop effective solutions, the feasibility is first investigated and found to be independent with EH constraints and PS factors. Based on this, we develop an effective initializing procedure for the design problems. Then, effective iterative solving algorithms are developed based on alternative optimization (AO) framework and semidefinite programming relaxation (SDR) techniques. Specifically, we find that the original problems can be equivalently reformulated as convex semidefinite programming (SDP) with respect to the transceivers and PS ratios when the receivers are fixed. On the other hand, when the transmitters and PS factors are fixed, the original problems degenerate to the classical linear MSE minimization receiver design problem for the BC network and the SINR maximization receiver design problem for the IC network, respectively. Since the SDP problems can be solved exactly in polynomial time, feasible solutions can be obtained for the proposed algorithms effectively.

However, the SDP solving is not computationally efficient for large number of variables case [10], and the computational complexity of the SDP-based algorithms is prohibitively high for large number of antenna and user. This greatly restricts its application. To break this, low-complexity schemes should be developed. In this chapter, closed-form power splitting factors with given the transceivers designed from traditional transceiver design algorithms are developed.

Notations: $\mathcal{C}$ represents the complex and positive real field. Bold uppercase and lowercase letters represent matrix and column vectors, respectively. Nonbold italic letters represent scalar values. $\mathbf{I}_N$ is an $N \times N$ identity matrix. $\mathbf{A}^{\mathrm{H}}$, $\mathbf{A}^{\mathrm{T}}$, and $\mathbf{A}^{-1}$ represent the Hermitian transpose, transpose, and inverse of $\mathbf{A}$, respectively. $\mathrm{Tr}(\mathbf{A})$ and $rank(\mathbf{A})$ are the trace and rank of matrix $\mathbf{A}$, respectively. $|\mathbf{A}|$ denotes the determinant of matrix $\mathbf{A}$. $\mathbf{A} = \mathrm{diag}(a_1, \dots, a_i, a_{i+1}, \dots, a_N)$ is a $N \times N$ diagonal matrix with the i-th diagonal elements being a_i. $\mathbb{E}[\cdot]$ denotes the statistical expectation. $\|\cdot\|_2$ and $\|\cdot\|_F$ denote the two-norm and Frobenius norm, respectively.

2. Joint transceiver design and power splitting optimization based on MSE criterion for MIMO BC channel

2.1 System model

A downlink MIMO BC channel network shown in **Figure 1**, where one base station (BS) serves K mobile stations (MSs) simultaneously through spatial multiplexing, is considered. The number of antennas of the BS and the kth ($k \in \{1, 2, \dots, K\}$) user are denoted as M and L_k, respectively. N_k represents the number of data stream for the kth user, and the total number of data streams served by BS is $d = \sum_{k=1}^{K} N_k \le M$. Let $\mathbf{s}_k \in \mathcal{C}^{N_k \times 1}$ denote the data vector transmitted to the user k, the data vector transmitted by BS can be expressed as $\mathbf{s} = \left[\mathbf{s}_1^H, \dots, \mathbf{s}_K^H\right]^H \in \mathcal{C}^{d \times 1}$. It is assumed that $\mathbb{E}\left[\mathbf{s}\mathbf{s}^{\mathrm{H}}\right] = \mathbf{I}_d$.

The BS transmits the signal $\mathbf{s}$ to users, and the received baseband signal at the kth receiver is

$$\mathbf{r}_k = \mathbf{H}_k \mathbf{G} \mathbf{s} + \mathbf{n}_k, \tag{1}$$

where $\mathbf{G} \in \mathcal{C}^{M \times d}$ denote the transmit precoding matrix, $\mathbf{H}_k \in \mathcal{C}^{L_k \times M}$ denotes the channel propagation matrix from the BS to the kth user and $\mathbf{n}_k \in \mathcal{C}^{L_k \times 1}$ denotes the noise vector, elements of which are assumed to be independent and identically (i.i.d.) zero mean complex Gaussian random variables with variance $\sigma^2_{\mathbf{n}_k}$. The total transmit power of the BS can be calculated as $P = \|\mathbf{G}\|_F^2$.

As shown in **Figure 1**, each user divides the received signal into two parts through power splitters, one part is for information decoder (ID) and the other is for EH. For easy analysis, solution, and implementation, we adopt the uniform PS model [11] in this chapter, that is, the power splitters of all the antennas of a user have the same PS factor. Denote $0 \le \rho_k \le 1$ as the PS factors for the kth user, the signal received at the ID of the kth user is

$$\mathbf{r}_k^{ID} = \sqrt{\rho_k}(\mathbf{H}_k \mathbf{G} \mathbf{s} + \mathbf{n}_k) + \mathbf{w}_k, \tag{2}$$

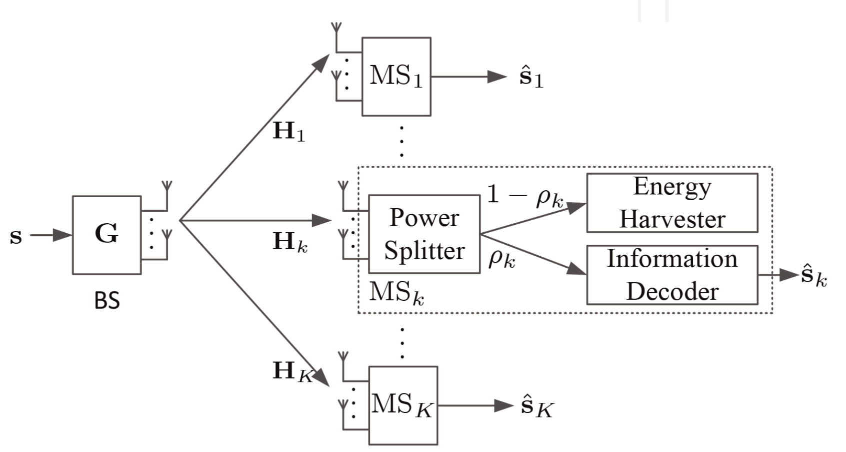

Figure 1.
Downlink MU-MIMO SWIPT system.

where $\mathbf{w}_k \in \mathcal{C}^{L_k \times 1}$ is the noise caused by power splitter, elements of which are assumed to be i.i.d. zero mean complex Gaussian random variables with variance $\sigma^2_{\mathbf{w}_k}$. The signal received by the EH receiver of user k is written as

$$\mathbf{r}_k^{EH} = \sqrt{1-\rho_k}(\mathbf{H}_k\mathbf{G}\mathbf{s} + \mathbf{n}_k). \tag{3}$$

At the ID receiver, a filter $\mathbf{F}_k \in \mathcal{C}^{N_k \times L_k}$ is employed to process the received signal and the detected signal is written as

$$\hat{\mathbf{s}}_k = \frac{1}{\sqrt{\rho_k}}\mathbf{F}_k\mathbf{r}_k^{ID} = \mathbf{F}_k\mathbf{H}_k\mathbf{G}\mathbf{s} + \mathbf{F}_k\mathbf{n}_k + \frac{1}{\sqrt{\rho_k}}\mathbf{F}_k\mathbf{w}_k. \tag{4}$$

It is noted that a scaling factor $\frac{1}{\sqrt{\rho_k}}$ is introduced to the received signal, which makes the problem modeling and solving more convenient.

Consequently, the MSE at the kth ID receiver can be expressed as

$$\begin{aligned}\mathrm{MSE_k} &= \mathbb{E}\left[\|\hat{\mathbf{s}}_\mathrm{k} - \mathbf{s}_\mathrm{k}\|_2^2\right] \\ &= \mathrm{Tr}(\mathbf{I}_{\mathrm{N_k}}) + \mathrm{Tr}\left(\mathbf{H}_\mathrm{k}^\mathrm{H}\mathbf{F}_\mathrm{k}^\mathrm{H}\mathbf{F}_\mathrm{k}\mathbf{H}_\mathrm{k}\mathbf{G}\mathbf{G}^\mathrm{H}\right) - \mathrm{Tr}\left(\boldsymbol{\Xi}_\mathrm{k}\mathbf{G}^\mathrm{H}\mathbf{H}_\mathrm{k}^\mathrm{H}\mathbf{F}_\mathrm{k}^\mathrm{H}\right) \\ &\quad -\mathrm{Tr}\left(\mathbf{F}_\mathrm{k}\mathbf{H}_\mathrm{kk}\mathbf{G}\boldsymbol{\Xi}_\mathrm{k}^\mathrm{H}\right) + \left(\sigma^2_{\mathbf{n}_\mathrm{k}} + \frac{\sigma^2_{\mathbf{w}_\mathrm{k}}}{\rho_\mathrm{k}}\right)\mathrm{Tr}\left(\mathbf{F}_\mathrm{k}^\mathrm{H}\mathbf{F}_\mathrm{k}\right).\end{aligned} \tag{5}$$

where $\boldsymbol{\Xi}_k = \left[\mathbf{0}_{N_k \times \sum_{l=1}^{k-1} N_l}, \mathbf{I}_{N_k}, \mathbf{0}_{N_k \times \sum_{l=k+1}^{K} N_l}\right]$. At the same time, the energy harvested by the kth EH receiver is expressed as

$$P_k^{\mathrm{EH}} = \xi_k(1-\rho_k)\left(\|\mathbf{H}_k\mathbf{G}\|_F^2 + L_k\sigma^2_{\mathbf{n}_k}\right), \tag{6}$$

where $0 \le \xi_k \le 1$ denotes the energy conversion efficiency.

2.2 Problem formulation and feasibility analysis

2.2.1 Problem formulation

A case that each MS has its dedicated ID and EH QoS requirements and the BS has to satisfy all the users with minimum transmit power consumed is considered. This scenario can be modeled by the following QoS constrained power minimization problem

$$\begin{aligned} \min_{\{\mathbf{G}, \mathbf{F}_k, \rho_k, \forall k\}} \quad & \mathrm{Tr}\left(\mathbf{G}\mathbf{G}^\mathrm{H}\right) \\ \text{s.t. :} \quad & \mathrm{MSE}_k \le \varepsilon_k, \\ & P_k^{\mathrm{EH}} \ge \psi_k, \\ & 0 < \rho_k < 1, \forall k = 1, \dots, K, \end{aligned} \tag{7}$$

where $\varepsilon_k > 0$ and $\psi_k > 0$ are the ID MSE target and the EH threshold of user k, respectively.

Obviously, (7) is nonconvex with respect to the precoders, receivers, and power splitters and thus difficult to be solved directly. Before developing an effective algorithm for it, its feasibility should be analyzed first.

DOI: http://dx.doi.org/10.5772/intechopen.89676

2.2.2 Feasibility analysis

Some sufficient and necessary conditions for the feasibility of the original problem (7) can be given by the following propositions.

Proposition 1 *Problem (7) is feasible if and only if the following problem is feasible:*

$$\begin{aligned} \min_{\{\mathbf{G},\mathbf{F}_k,\rho_k,\forall k\}} \quad & \mathrm{Tr}\left(\mathbf{G}\mathbf{G}^{\mathrm{H}}\right) \\ \text{s.t.}: \; & \|\mathbf{F}_k\mathbf{H}_k\mathbf{G}-\boldsymbol{\Xi}_k\|_{\mathrm{F}}^2+\left(\sigma_{\mathbf{n}_k}^2+\frac{\sigma_{\mathbf{w}_k}^2}{\rho_k}\right)\|\mathbf{F}_k\|_{\mathrm{F}}^2\le\varepsilon_k, \\ & \forall k=1,\ldots,K. \end{aligned} \tag{8}$$

Proposition 2 *Problem (8) is feasible if and only if the following problem is feasible:*

$$\begin{aligned} \min_{\{\mathbf{G},\mathbf{F}_k,\forall k\}} \quad & \mathrm{Tr}\left(\mathbf{G}\mathbf{G}^{\mathrm{H}}\right) \\ \text{s.t.}: \; & \|\mathbf{F}_k\mathbf{H}_k\mathbf{G}-\boldsymbol{\Xi}_k\|_{\mathrm{F}}^2+\left(\sigma_{\mathbf{n}_k}^2+\sigma_{\mathbf{w}_k}^2\right)\|\mathbf{F}_k\|_{\mathrm{F}}^2\le\varepsilon_k, \\ & \forall k=1,\ldots,K. \end{aligned} \tag{9}$$

For the sake of brevity, we omit the proof to these propositions. Interested readers are suggested to refer to [12–16]. Proposition 1 reveals that the feasibility of the original problem (7) is irrelevant to the EH constraints, while Proposition 2 further shows that the EH constraints are irrelevant to the feasibility. Since the feasibility of the formulated problem depends on neither the EH constraints nor the PS factors, checking its feasibility can be simplified to checking the feasibility of (9), which is a traditional MSE-based multiuser MIMO transceiver design problem [17–19]. So, in the following, we assume that problem (9) is feasible under the given MSE QoS requirements and focus on how to solve it.

2.3 Alternative optimization solution based on semidefinite programming relaxation

2.3.1 Alternative optimization framework

By reviewing the MSE expression (5), we know that it is convex with respect to either $\mathbf{G}$ or $\mathbf{F}_k$. So, we can develop an iterative algorithm for the original problem based on the optimization (AO) framework, that is, optimizing the transmit precoder together with PS factors and the receivers iteratively.

Specifically, when the receiver $\mathbf{F}_k, \forall k$ is fixed, the optimization problem is reduced to a joint transmitter design and power splitting (JTDPS) subproblem, which is

$$\begin{aligned} \min_{\{\mathbf{G},\rho_k,\forall k\}} \quad & \mathrm{Tr}\left(\mathbf{G}\mathbf{G}^{\mathrm{H}}\right) \\ \text{s.t.}: \quad & \mathrm{MSE}_k\le\varepsilon_k, \\ & P_k^{\mathrm{EH}}\ge\psi_k, \\ & 0\le\rho_k\le 1,\forall k=1,\ldots,K. \end{aligned} \tag{10}$$

It is noted that problem (10) is not convex in its current form. We will further process it based on SDR techniques in the next subsection.

When the precoders and PS factors are fixed, the transmit power at the BS and the EH power are fixed. Considering that only MSE at the ID receiver of user k is relevant to $\mathbf{F}_k$, we can optimize the ID receiver by minimizing the MSE. The optimization problem can be formulated as

$$\min_{\{\mathbf{F}_k\}} \quad \mathrm{MSE}_k. \tag{11}$$

Problem (11) is the traditional unconstrained MSE minimization problem and its closed-form solution can be given by

$$\mathbf{F}_k = \left(\mathbf{H}_k\mathbf{G}\boldsymbol{\Xi}_k^{\mathrm{H}}\right)^{\mathrm{H}}\left[\mathbf{H}_k\mathbf{G}\mathbf{G}^{\mathrm{H}}\mathbf{H}_k^{\mathrm{H}} + \left(\sigma_{\mathbf{n}_k}^2 + \frac{\sigma_{\mathbf{w}_k}^2}{\rho_k}\right)\mathbf{I}\right]^{-1}. \tag{12}$$

Therefore, by alternatively optimizing the transmitter together with PS factors according to (10) and the receivers according to (12), an iterative optimization framework is established and is summarized in Algorithm 1.

Algorithm 1 Alternating optimization framework for JTDPS.

1: Initialize the receivers $\mathbf{F}_k = \tilde{\mathbf{F}}_k, \forall k$ and the power splitting factors $\rho_k, \ \forall k$.
2: Optimize the transmitter $\mathbf{G}$ and the PS factors $\rho_k, \forall k$ by solving problem (10).
3: Optimize the receive filters $\mathbf{F}_k, \forall k$ according to (12).
4: Repeat 2 and 3 until convergence or the maximum number of iterations is reached.

2.3.2 Convergence analysis

For the AO framework, it is vital to analyze its convergence property. The following proposition reveals this property.

Proposition 3 For the initial receivers $\tilde{\mathbf{F}}_k, \forall k$, if problem (10) is feasible and its optimal solution can be obtained, then the proposed Algorithm 1 is convergent.

The proof can be found in [12]. According to Proposition 3, two critical prerequisites should be satisfied in order to guarantee finding a feasible solution for problem (7) through Algorithm 1. 1) the subproblem (10) should be feasible and 2) the initialization of the receivers $\mathbf{F}_k, \forall k$ should be carefully chosen such that proper transmitters and the PS factors can be obtained in the first iteration of the Algorithm 1. This means that it is vital to find the optimal solution for the subproblem (10). Therefore, before proceeding, the feasibility of the subproblem (10) is investigated in the following subsection.

2.3.3 Feasibility of the transmitter design subproblem

By checking the MSE constraints of (9), a necessary condition for the feasibility of problem (9) is established as

$$\varepsilon_k - \left(\sigma_{\mathbf{n}_k}^2 + \sigma_{\mathbf{w}_k}^2\right)\|\mathbf{F}_k\|_{\mathrm{F}}^2 \geq 0. \tag{13}$$

This condition shows that the Frobenius norm of the receiver should be small enough to make the problem feasible. In order to satisfy this condition, we introduce a positive scaling parameter p_k to the receiver $\mathbf{F}_k$ in the transceiver design model (10), that is, $\frac{1}{p_k}\mathbf{F}_k$. The expression of MSE is then recast as

$$\mathrm{MSE}_k = \|\frac{1}{p_k}\mathbf{F}_k\mathbf{H}_k\mathbf{G} - \boldsymbol{\Xi}_k\|_\mathrm{F}^2 + \left(\sigma_{\mathbf{n}_k}^2 + \frac{\sigma_{\mathbf{w}_k}^2}{\rho_k}\right)\frac{\|\mathbf{F}_k\|_\mathrm{F}^2}{p_k^2} \tag{14}$$

After replacing the MSE constraints with (14), problem (10) can then be reformulated as

$$\begin{aligned} \min_{\{\mathbf{G}, p_k, \rho_k, \forall k\}} \quad & \mathrm{Tr}\left(\mathbf{G}\mathbf{G}^\mathrm{H}\right) \\ \text{s.t.}: \quad & \left\|\frac{1}{p_k}\mathbf{F}_k\mathbf{H}_k\mathbf{G} - \boldsymbol{\Xi}_k\right\|_\mathrm{F}^2 + \left(\sigma_{\mathbf{n}_k}^2 + \frac{\sigma_{\mathbf{w}_k}^2}{\rho_k}\right)\frac{1}{p_k^2}\|\mathbf{F}_k\|_\mathrm{F}^2 \le \varepsilon_k, \\ & \xi_k(1-\rho_k)\left(\|\mathbf{H}_k\mathbf{G}\|_\mathrm{F}^2 + L_k\sigma_{\mathbf{n}_k}^2\right) \ge \psi_k, \\ & \forall k = 1, \dots, K. \end{aligned} \tag{15}$$

It can be proved that a sufficient and necessary condition for the feasibility of problem (15) is given by the following proposition [12].

Proposition 4 Problem (15) is feasible if and only if the following problem is feasible:

$$\begin{aligned} \min_{\{\mathbf{G}, p_k, \forall k\}} \quad & \mathrm{Tr}\left(\mathbf{G}\mathbf{G}^\mathrm{H}\right) \\ \text{s.t.}: \quad & \left\|\frac{1}{p_k}\mathbf{F}_k\mathbf{H}_k\mathbf{G} - \boldsymbol{\Xi}_k\right\|_\mathrm{F}^2 + \left(\sigma_{\mathbf{n}_k}^2 + \sigma_{\mathbf{w}_k}^2\right)\frac{1}{p_k^2}\|\mathbf{F}_k\|_\mathrm{F}^2 \le \varepsilon_k, \\ & \forall k = 1, \dots, K. \end{aligned} \tag{16}$$

Proposition 4 reveals that the feasibility of the transmitter and PS problem (15) does not depend on the EH constraints either. Therefore, the feasibility of the joint transmitter design and PS problem (15) can be simply verified by checking whether problem (16) is feasible or not. To guarantee the feasibility of problem (16), the following proposition is proposed.

Proposition 5 Fix $\mathbf{F}_k, \forall k$, problem (16) can be reformulated as a convex SDP problem given by

$$\begin{aligned} \min_{\{\mathbf{G}, p_k, \forall k\}} \quad & \|\mathbf{G}\|_\mathrm{F}^2 \\ \text{s.t.}: \quad & \begin{bmatrix} p_k\sqrt{\varepsilon} & \mathbf{a}_k^\mathrm{H} & \beta_k \\ \mathbf{a}_k & p_k\sqrt{\varepsilon}\mathbf{I} & \mathbf{0} \\ \beta_k & \mathbf{0} & p_k\sqrt{\varepsilon} \end{bmatrix} \succeq \mathbf{0}, \forall k = 1, \dots, K, \end{aligned} \tag{17}$$

where $\beta_k = \sqrt{\sigma_{\mathbf{n}_k}^2 + \sigma_{\mathbf{w}_k}^2}\|\mathbf{F}_k\|_\mathrm{F}$, and $\mathbf{a}_k = \mathrm{vec}\left(\mathbf{F}_k\mathbf{H}_k\mathbf{G} - p_k\boldsymbol{\Xi}_k\right)$ is affine jointly in $\mathbf{G}$ and p_k.

Proof. The MSE constraints in problem (16) can be recast as

$$\begin{aligned} p_k^2\mathrm{MSE}_k &= \left\|\mathbf{F}_k\mathbf{H}_k\mathbf{G} - p_k\boldsymbol{\Xi}_k\right\|_\mathrm{F}^2 + \left(\sigma_{\mathbf{n}_k}^2 + \sigma_{\mathbf{w}_k}^2\right)\|\mathbf{F}_k\|_\mathrm{F}^2 \\ &= \|\mathrm{vec}\left(\mathbf{F}_k\mathbf{H}_k\mathbf{G} - p_k\boldsymbol{\Xi}_k\right)\|_2^2 + \left(\sigma_{\mathbf{n}_k}^2 + \sigma_{\mathbf{w}_k}^2\right)\|\mathbf{F}_k\|_\mathrm{F}^2 \\ &= \left\|\begin{bmatrix} \mathbf{a}_k \\ \beta_k \end{bmatrix}\right\|_2^2 \le p_k^2\varepsilon \end{aligned} \tag{18}$$

1: Given the MSE requirements $\varepsilon_k, \forall k$.
2: Generate random matrix $\tilde{\mathbf{F}}_k \in \mathbf{C}^{M\times N}, \forall k$.
3: By fixing $\mathbf{F}_k = \tilde{\mathbf{F}}_k$, solve (17) to obtain the optimized receivers $\mathbf{G}$ and PS factors $p_k, \forall k$.
4: Return $\mathbf{F}_k = \frac{1}{p_k}\tilde{\mathbf{F}}_k, \forall k$.

Table 1.
The initializing procedure for algorithm 1.

According to the Schur complement lemma, the inequality (18) is equivalent to

$$\begin{bmatrix} p_k\sqrt{\varepsilon} & \mathbf{a}_k^{\mathrm{H}} & \beta_k \\ \mathbf{a}_k & p_k\sqrt{\varepsilon}\mathbf{I} & \mathbf{0} \\ \beta_k & \mathbf{0} & p_k\sqrt{\varepsilon} \end{bmatrix} \succeq \mathbf{0}. \tag{19}$$

The proposition is obtained.

Problem (17) is convex, and its optimal solution can be obtained. Therefore, problem (16) is feasible. With the solution of problem (16), an effective initialization procedure for problem (16) can be constructed. Specifically, the receiver $\mathbf{F}_k$ can be initialized by any randomly generated matrix, that is, $\mathbf{F}_k = \tilde{\mathbf{F}}_k \in \mathcal{C}^{L_k\times M}, \forall k$. Then, by solving (17), p_k is obtained. Finally, the receiver $\mathbf{F}_k$ is constructed to be $\frac{1}{p_k}\tilde{\mathbf{F}}_k$, such that the problem (16) is feasible. The initialization process is summarized in **Table 1**.

Through Proposition 4 and Proposition 5, it is known that the joint transmitter design and power splitting subproblem is feasible. However, Algorithm 1 cannot be carried out in its current form, since problem (10) is still nonconvex. In the following, the SDP relaxation is adopted to reform it in to convex form.

2.3.4 Algorithm description

By introducing two variables c_k and d_k with $\frac{\sigma^2_{\mathbf{w}_k}}{\rho_k} \le c_k$ and $\frac{\psi_k}{\xi_k(1-\rho_k)} \le d_k, \forall k = 1, \ldots, K$, (10) can be rewritten as

$$\begin{aligned} \min_{\{\mathbf{G},\rho_k,c_k,d_k,\forall k\}} \quad & \mathrm{Tr}\left(\mathbf{G}\mathbf{G}^{\mathrm{H}}\right) \\ \text{s.t.}: \; & \mathrm{Tr}\left(\mathbf{G}^{\mathrm{H}}\mathbf{H}_k^{\mathrm{H}}\mathbf{F}_k^{\mathrm{H}}\mathbf{F}_k\mathbf{H}_k\mathbf{G}\right) - \mathrm{Tr}\left(\boldsymbol{\Xi}_k\mathbf{G}^{\mathrm{H}}\mathbf{H}_k^{\mathrm{H}}\mathbf{F}_k^{\mathrm{H}}\right) - \mathrm{Tr}\left(\mathbf{F}_k\mathbf{H}_{kk}\mathbf{G}\mathrm{X}_k^{\mathrm{H}}\right) \\ & + \left(\sigma^2_{\mathbf{n}_k} + c_k\right)\mathrm{Tr}\left(\mathbf{F}_k^{\mathrm{H}}\mathbf{F}_k\right) \le \varepsilon_k - N_k, \\ & \mathrm{Tr}\left(\mathbf{G}^{\mathrm{H}}\mathbf{H}_k^{\mathrm{H}}\mathbf{H}_k\mathbf{G}\right) + L_k\sigma^2_{\mathbf{n}_k} \ge d_k, \\ & \frac{\sigma^2_{\mathbf{w}_k}}{\rho_k} \le c_k, \\ & \frac{\psi_k}{\xi_k(1-\rho_k)} \le d_k, \\ & 0 \le \rho_k \le 1, \forall k = 1, \ldots, K. \end{aligned} \tag{20}$$

Adopting the Schur complement lemma, the constraints $\frac{\sigma^2_{\mathbf{w}_k}}{\rho_k} \le c_k$ and $\frac{\psi_k}{\xi_k(1-\rho_k)} \le d_k$ can be reformulated as $\begin{bmatrix} c_k & \sigma_w \\ \sigma_w & \rho_k \end{bmatrix} \succeq \mathbf{0}$ and $\begin{bmatrix} d_k & \sqrt{\psi_k/\xi_k} \\ \sqrt{\psi_k/\xi_k} & 1-\rho_k \end{bmatrix} \succeq \mathbf{0}$, respectively. Then, problem (21) can be further rewritten as

$$
\begin{aligned}
&\min_{\{\mathbf{G},\rho_k,c_k,d_k,\forall k\}} \quad \mathrm{Tr}\left(\mathbf{G}\mathbf{G}^{\mathrm{H}}\right)\\
&\text{s.t.}: \mathrm{Tr}\left(\mathbf{G}^{\mathrm{H}}\mathbf{H}_k^{\mathrm{H}}\mathbf{F}_k^{\mathrm{H}}\mathbf{F}_k\mathbf{H}_k\mathbf{G}\right) - \mathrm{Tr}\left(\boldsymbol{\Xi}_k\mathbf{G}^{\mathrm{H}}\mathbf{H}_k^{\mathrm{H}}\mathbf{F}_k^{\mathrm{H}}\right) - \mathrm{Tr}\left(\mathbf{F}_k\mathbf{H}_{kk}\mathbf{G}\boldsymbol{\Xi}_k^{\mathrm{H}}\right)\\
&\quad +\left(\sigma_{\mathbf{n}_k}^2 + c_k\right)\mathrm{Tr}\left(\mathbf{F}_k^{\mathrm{H}}\mathbf{F}_k\right) \le \varepsilon_k - N_k,\\
&\quad \mathrm{Tr}\left(\mathbf{G}^{\mathrm{H}}\mathbf{H}_k^{\mathrm{H}}\mathbf{H}_k\mathbf{G}\right) + L_k\sigma_{\mathbf{n}_k}^2 \ge d_k,\\
&\quad \begin{bmatrix} c_k & \sigma_w \\ \sigma_w & \rho_k \end{bmatrix} \succeq \mathbf{0},\\
&\begin{bmatrix} d_k & \sqrt{\psi_k/\xi_k} \\ \sqrt{\psi_k/\xi_k} & 1-\rho_k \end{bmatrix} \succeq \mathbf{0},\\
&0 \le \rho_k \le 1, \forall k = 1, \dots, K.
\end{aligned}
\tag{21}
$$

Problem (21) is a nonconvex inhomogeneous quadratically constrained quadratic program (QCQP) [20, 21], which are NP-hard [10, 22–25]. In order to solve it effectively, SDR is utilized. Specifically, a new variable $\mathbf{X} = \mathbf{G}\mathbf{G}^{\mathrm{H}}$ is defined and relaxed as $\mathbf{X} \succeq \mathbf{G}\mathbf{G}^{\mathrm{H}}$, which is equivalent to $\begin{bmatrix} \mathbf{X} & \mathbf{G} \\ \mathbf{G}^H & \mathbf{I}_d \end{bmatrix} \succeq \mathbf{0}$, problem (21) can be relaxed as

$$
\begin{aligned}
&\min_{\{\mathbf{X}\succeq\mathbf{0},\mathbf{G},\rho_k,c_k,d_k,\forall k\}} \quad \mathrm{Tr}(\mathbf{X})\\
&\text{s.t.}: \mathrm{Tr}\left(\mathbf{H}_k^{\mathrm{H}}\mathbf{F}_k^{\mathrm{H}}\mathbf{F}_k\mathbf{H}_k\mathbf{X}\right) - \mathrm{Tr}\left(\mathbf{G}^{\mathrm{H}}\mathbf{H}_k^{\mathrm{H}}\mathbf{F}_k^{\mathrm{H}}\boldsymbol{\Xi}_k\right) - \mathrm{Tr}\left(\boldsymbol{\Xi}_k^{\mathrm{H}}\mathbf{F}_k\mathbf{H}_{kk}\mathbf{G}\right) + \left(\sigma_{\mathbf{n}_k}^2 + c_k\right)\mathrm{Tr}\left(\mathbf{F}_k^{\mathrm{H}}\mathbf{F}_k\right) \le \varepsilon_k - N_k,\\
&\quad \mathrm{Tr}\left(\mathbf{H}_k^{\mathrm{H}}\mathbf{H}_k\mathbf{X}\right) + L_k\sigma_{\mathbf{n}_k}^2 \ge d_k,\\
&\quad \begin{bmatrix} c_k & \sigma_w \\ \sigma_w & \rho_k \end{bmatrix} \succeq \mathbf{0},\\
&\quad \begin{bmatrix} d_k & \sqrt{\psi_k/\xi_k} \\ \sqrt{\psi_k/\xi_k} & 1-\rho_k \end{bmatrix} \succeq \mathbf{0},\\
&\quad 0 \le \rho_k \le 1, \forall k = 1, \dots, K,\\
&\quad \begin{bmatrix} \mathbf{X} & \mathbf{G} \\ \mathbf{G}^H & \mathbf{I}_d \end{bmatrix} \succeq \mathbf{0}.
\end{aligned}
\tag{22}
$$

Problem (22) is a convex SDP with respect to $\mathbf{G} \in \mathcal{C}^{M\times d}$, positive semidefinite Hermitian symmetric variable $\mathbf{X} \in \mathcal{C}^{M\times M}$ and nonnegative variables $\rho_k, c_k, d_k, \forall k$ and thus can be solved efficiently by using traditional convex optimization techniques [23, 26].

It is noted that the optimal objective of (22) is a lower bound of that of the nonconvex QCQP problem (21), since the same objective function is minimized over a larger set [27]. Let $\mathbf{X}_{\mathrm{SDR}}$ and $\mathbf{G}_{\mathrm{SDR}}$ denote the optimal solution of the SDR problem (22), if $\mathbf{X}_{SDR} = \mathbf{G}_{SDR}\mathbf{G}_{SDR}^{\mathrm{H}}$, then $\mathbf{G}_{\mathrm{SDR}}$ must be optimal for (21). Although not yet proven, simulation results show that the relaxation is always tight, that is, the equality in the relaxation is always satisfied. Replacing $\mathbf{G}$ in step 2 of Algorithm 1 with $\mathbf{G}_{\mathrm{SDR}}$ results in an SDP-based JTDPS (SDP-JTDPS) algorithm, a practical algorithm solving problem (10) is finally obtained.

The complexity of Algorithm 1 is mainly introduced by the SDP (22). Given a solution accuracy $\epsilon > 0$, the computational complexity solving SDP is about

$\mathcal{O}\left(N_{\text{Iter}}M^{4.5}\log\left(1/\epsilon\right)\right)$ [10], where N_{Iter} is the iteration number. Therefore, the computational complexity of the algorithm is prohibitively high when the system becomes large in number of antennas and users. So, it is necessary to develop low-complexity algorithms.

2.4 Low-complexity design scheme

In this section, a low-complexity algorithm is derived by first designing ID transceivers to satisfy the MSE constraints and then optimizing the transmit power together with PS factors with the designed transceivers. The scheme is of quite low computational complexity.

It is noted that the MSE-constrained transceiver design problem (9) can be solved efficiently by existing methods proposed in [17]. So, let $\left\{\hat{\mathbf{G}}, \hat{\mathbf{F}}_k, \forall k\right\}$ denote its solution, amplify the precoder $\hat{\mathbf{G}}$ by a positive scaling factor $\sqrt{\alpha} > 1$, and decrease the receiver $\hat{\mathbf{F}}_k$ by the factor $1/\sqrt{\alpha}$, the problem (9) can be rewritten as

$$\begin{aligned}
&\min_{\{\alpha, \rho_k, \forall k\}} \quad \alpha \mathrm{Tr}\left(\hat{\mathbf{G}}\hat{\mathbf{G}}^{\mathrm{H}}\right) \\
&\text{s.t. : } \left\|\hat{\mathbf{F}}_k\mathbf{H}_k\hat{\mathbf{G}} - \boldsymbol{\Xi}_k\right\|_{\mathrm{F}}^2 + \left(\sigma_{\mathbf{n}_k}^2 + \frac{\sigma_{\mathbf{w}_k}^2}{\rho_k}\right)\frac{1}{\alpha}\left\|\hat{\mathbf{F}}_k\right\|_{\mathrm{F}}^2 \le \varepsilon_k, \\
&\xi_k(1-\rho_k)\left(\alpha\|\hat{\mathbf{H}}_k\hat{\mathbf{G}}\|_F^2 + L_k\sigma_{\mathbf{n}_k}^2\right) \ge \psi_k, \\
&\alpha > 1, \\
&0 \le \rho_k \le 1, \\
&\forall k = 1, \dots, K,
\end{aligned} \tag{23}$$

where the scaling factor α and the PS factors in (7) are jointly optimized to satisfy both the MSE and EH constraints. Problem (23) can be solved in closed form, which is shown by the following proposition.

Proposition 6 The optimal solution of problem (23) is given in closed form by

$$\alpha^* = \max_{\forall k} \alpha_k^*, \tag{24}$$

$$\rho_k^* = \frac{\sigma_{\mathbf{w}_k}^2}{\alpha^* c_k - \sigma_{\mathbf{n}_k}^2}, \tag{25}$$

where $\alpha_k^* = \frac{B_k + \sqrt{B_k^2 - 4A_kC_k}}{2A_k}$ with $c_k = \frac{\varepsilon_k - \left\|\hat{\mathbf{F}}_k\mathbf{H}_k\hat{\mathbf{G}} - \boldsymbol{\Xi}_k\right\|_{\mathrm{F}}^2}{\left\|\hat{\mathbf{F}}_k\right\|_{\mathrm{F}}^2}$, $d_k = \|\hat{\mathbf{H}}_k\hat{\mathbf{G}}\|_F^2$, $A_k = c_k\xi_k d_k$, $B_k = \xi_k d_k\left(\sigma_{\mathbf{n}_k}^2 + \sigma_{\mathbf{w}_k}^2\right) + c_k\psi_k - c_k\xi_k L_k\sigma_{\mathbf{n}_k}^2$, and $C_k = \psi_k\sigma_{\mathbf{n}_k}^2 - \xi_k L_k\sigma_{\mathbf{n}_k}^2\left(\sigma_{\mathbf{n}_k}^2 + \sigma_{\mathbf{w}_k}^2\right)$.

Proof. Problem(23) can be transformed to

$$\min_{\{\alpha, \rho_k, \forall k\}} \quad \alpha \tag{26}$$

$$\text{s.t. : } \rho_k \ge \frac{\sigma_{\mathbf{w}_k}^2}{\alpha c_k - \sigma_{\mathbf{n}_k}^2}, \tag{27}$$

$$1 - \rho_k \ge \frac{\psi_k}{\xi_k\left(\alpha d_k + L_k\sigma_{\mathbf{n}_k}^2\right)}, \tag{28}$$

$$\alpha > 1, \tag{29}$$

$$0 < \rho_k < 1, \forall k = 1, \dots, K. \tag{30}$$

By summing (27) and (28) for user k, problem (26–30) is equivalent to

$$\begin{aligned} \min_{\{\alpha\}} \quad & \alpha \\ \text{s.t.}: \ & F_k(\alpha) \le 1, \forall k = 1, \dots, K, \\ & \alpha > 1, \end{aligned} \tag{31}$$

where $F_k(\alpha) = \frac{\sigma^2_{\mathbf{w}_k}}{\alpha c_k - \sigma^2_{\mathbf{n}_k}} + \frac{\psi_k}{\xi_k\left(\alpha d_k + L_k\sigma^2_{\mathbf{n}_k}\right)}$. Since the MSE constraints are satisfied with equality when $\alpha = 1$, there exists $\frac{\sigma^2_{\mathbf{w}_k}}{c_k - \sigma^2_{\mathbf{n}_k}} = 1$ or $\sigma^2_{\mathbf{w}_k} + \sigma^2_{\mathbf{n}_k} = c_k$, and $F_k(1) = 1 + \frac{\psi_k}{\xi_k\left(d_k + L_k\sigma^2_{\mathbf{n}_k}\right)} > 1$. It is known that $F_k(\alpha)$ will monotonically decrease when $\alpha > \frac{\sigma^2_{\mathbf{n}_k}}{c_k} = \frac{\sigma^2_{\mathbf{n}_k}}{\sigma^2_{\mathbf{n}_k} + \sigma^2_{\mathbf{w}_k}}$. Thus, $F_k(\alpha)$ decreases monotonically when $\alpha > 1$.

When $\alpha > 1$, the function $F_k(\alpha) = 1$ has a unique solution $\alpha_k^* = \frac{B_k + \sqrt{B_k^2 - 4A_kC_k}}{2A_k}$. Problem (31) is then equivalent to

$$\begin{aligned} \min_{\{\alpha\}} \quad & \alpha \\ \text{s.t.}: \ & \alpha \ge \alpha_k^*, \forall k. \end{aligned} \tag{32}$$

The optimal solution of problem (32) is given by $\alpha^* = \max_{\forall k} \alpha_k^*$.

For the optimal α^*, $F_k(\alpha^*) = \frac{\sigma^2_{\mathbf{w}_k}}{\alpha^* c_k - \sigma^2_{\mathbf{n}_k}} + \frac{\psi_k}{\xi_k\left(\alpha^* d_k + L_k\sigma^2_{\mathbf{n}_k}\right)} \le 1$. Let $\rho_k^* = \frac{\sigma^2_{\mathbf{w}_k}}{\alpha^* c_k - \sigma^2_{\mathbf{n}_k}}$, we have $\frac{\psi_k}{\xi_k\left(\alpha^* d_k + L_k\sigma^2_{\mathbf{n}_k}\right)} \le 1 - \rho_k^*$. Thus, $\left\{\alpha^*, \rho_k^*, \forall k\right\}$ is an optimal solution for (26–30).

Given α^* and $\left\{\hat{\mathbf{G}}, \hat{\mathbf{F}}_k, \forall k\right\}$, the transceiver which is feasible to problem (7) can be determined by $\left\{\mathbf{G} = \sqrt{\alpha^*}\hat{\mathbf{G}}, \mathbf{F}_k = \frac{1}{\sqrt{\alpha^*}}\hat{\mathbf{F}}_k, \forall k\right\}$. The design process is summarized in Algorithm 2.

Algorithm 2 Low-complexity closed-form PS (CF-PS) algorithm.

1: Solve problem (9) to obtain $\left\{\hat{\mathbf{G}}, \hat{\mathbf{F}}_k, \forall k\right\}$ based on the traditional MSE QoS constraint power minimization algorithm proposed in [17].
2: Optimize the optimal scaling factor α^* and the PS factors ρ_k^* according to (24) and (25).
3: Return the feasible solution $\left\{\mathbf{G} = \sqrt{\alpha^*}\hat{\mathbf{G}}, \mathbf{F}_k = \frac{1}{\sqrt{\alpha^*}}\hat{\mathbf{F}}_k, \rho_k^*, \forall k\right\}$ to problem (7).

The main computational complexity of Algorithm 2 comes from solving problem (9), which is of $\mathcal{O}\left(N_{\text{Iter}}d^3\right)$ [17]. Thus, the complexity of Algorithm 2 is quite lower than that of Algorithm 1.

2.5 Simulation results and analysis

The performance of the described algorithms is validated through simulations. The user number is set to be $K = 3$. The channel matrices $\mathbf{H}_k, \forall k$ are set as i.i.d. zero mean complex Gaussian random variables with variance $r_k^{-\beta}$, where r_k is the distance in meter between the jth transmitter and the kth receiver, and β is the path loss factor. The following parameters are set unless otherwise noted, $M = 8$, $L_k = L = 4$, $N_k = N = L/2$, $r_k = r = 5$, $\beta = 2.7$, $\sigma^2_{\mathbf{n}_k} = \sigma^2_n = 10^{-3}$, and $\sigma^2_{\mathbf{w}_k} = \sigma^2_w = 10^{-2}$. The MSE and EH thresholds are set nonuniformly as $\varepsilon_1 = 0.01$, $\varepsilon_2 = 0.02$, $\varepsilon_3 = 0.2$, $\psi_1 = 20$, $\psi_2 = 25$, and $\psi_3 = 30$dBm. CVX toolbox [26] is adopted to solve SDP problems. The traditional MSE QoS constraint (MSE-QoS-TRAD) power minimization algorithm [17] is adopted as a performance benchmark.

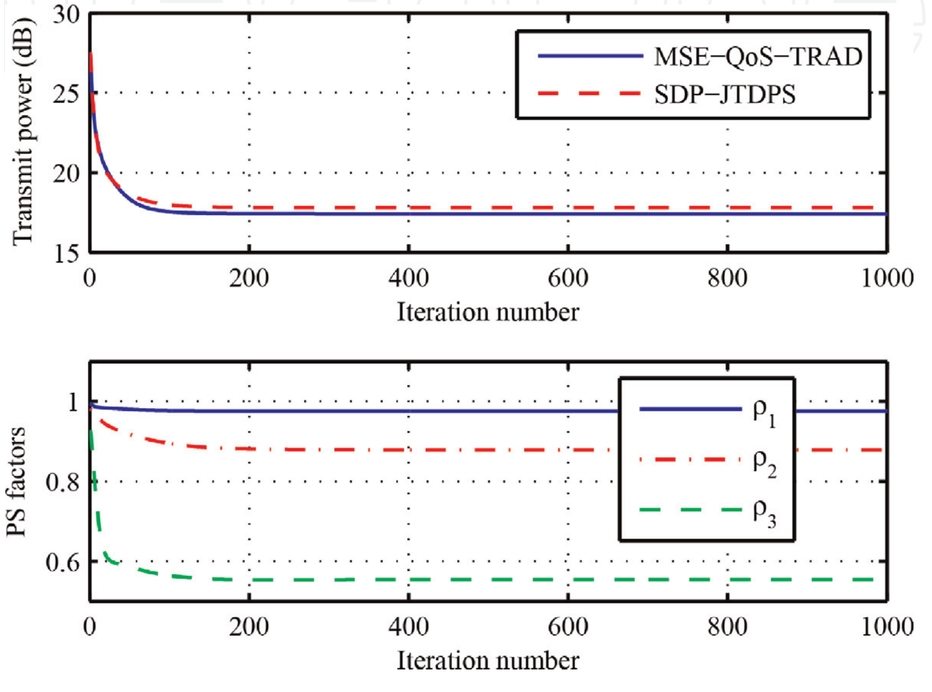

Figure 2.
Transmit power and PS factors versus iterations with the SDP-JTDPS algorithm.

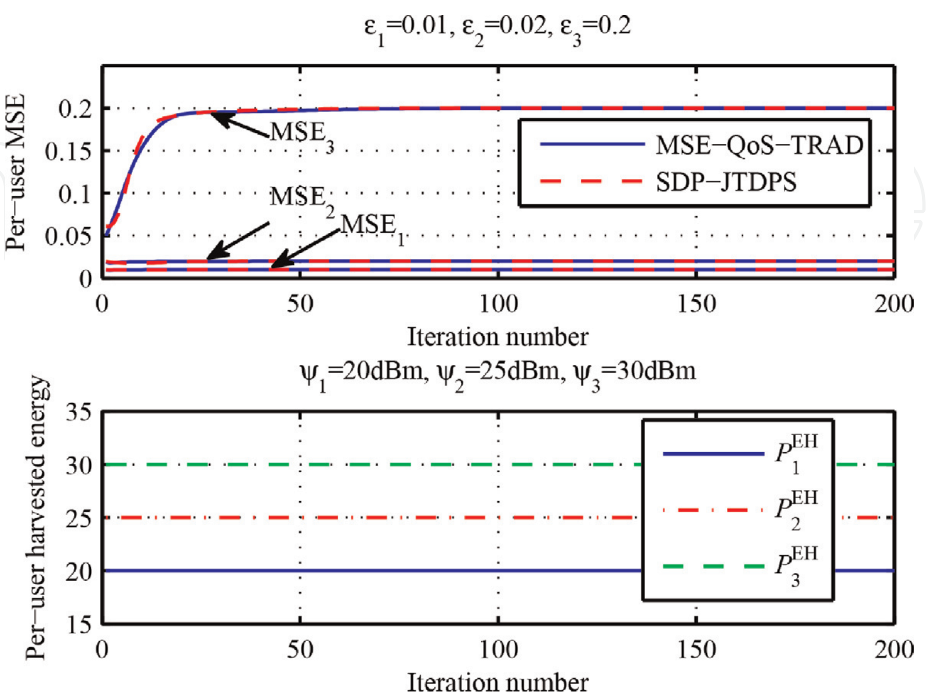

Figure 3.
Achieved per-user MSE and harvested energy versus iterations by the proposed SDP-TDPS scheme. The titles show the QoS targets.

The convergence property of the described scheme is shown in **Figure 2**. It can be seen that the optimized transmit power and the PS factors decrease monotonically along with the increase of the number of iterations. It needs special explanation that $\mathbf{X}_{\mathrm{SDR}} = \mathbf{G}_{\mathrm{SDR}}\mathbf{G}_{\mathrm{SDR}}^{\mathrm{H}}$ is always satisfied during the simulations. This verifies that the SDP solution of the relaxed problem (22) is also optimal for the joint transmitter and PS subproblem (10).

Figure 3 shows the per-user MSE and harvested energy of the proposed scheme along with iterations. Similar to the MSE-QoS-TRAD scheme, the SDP-JTDPS scheme satisfies the MSE QoS requirements in each iteration. Moreover, the EH requirements can also be satisfied.

The performance of SDP-JTDPS and CF-PS algorithms are compared in **Figure 4**. It can be observed that all of them achieve the MSE QoS requirements exactly. This is consistent with the analysis that the MSE constraints can be satisfied

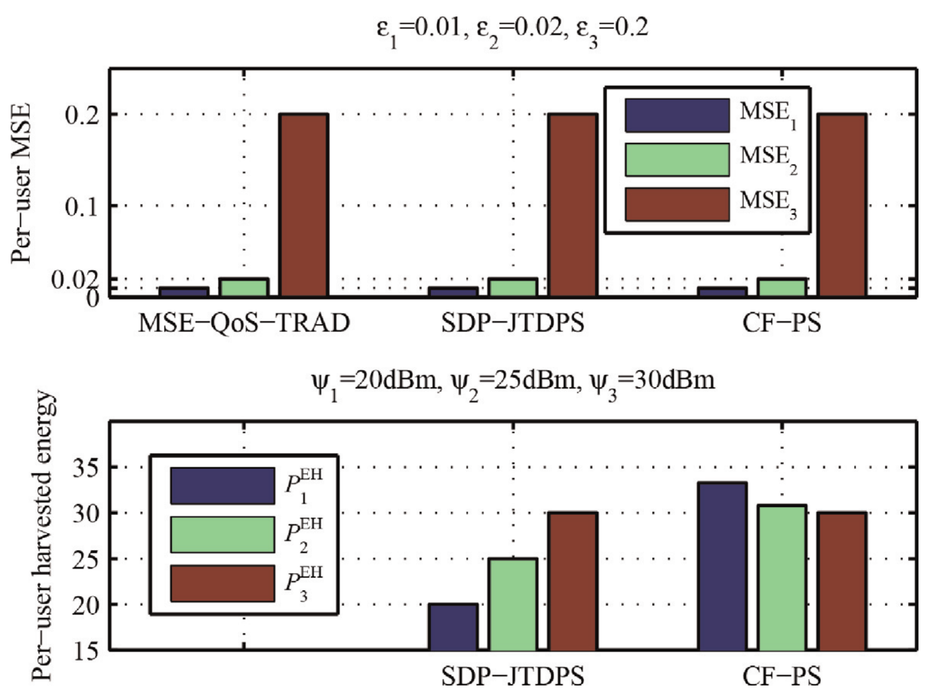

Figure 4.
Comparison of per-user MSE and harvested energy achieved by the proposed algorithms. The titles show the QoS targets.

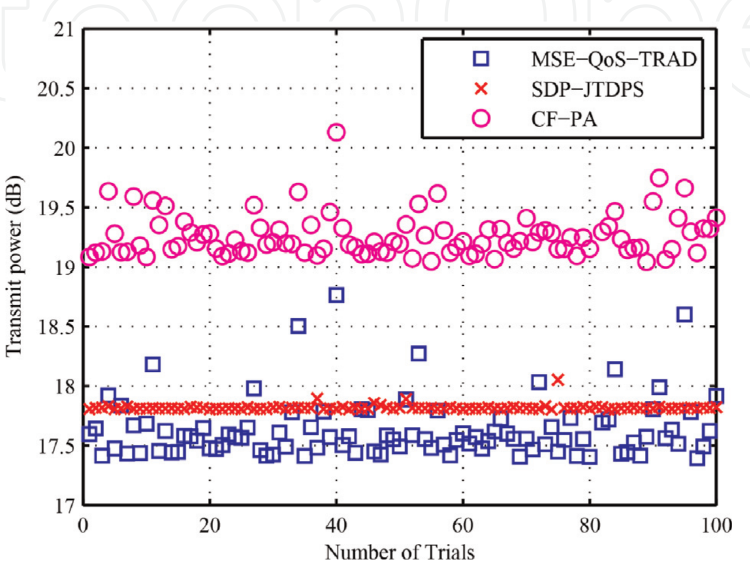

Figure 5.
Transmit power versus number of trials.

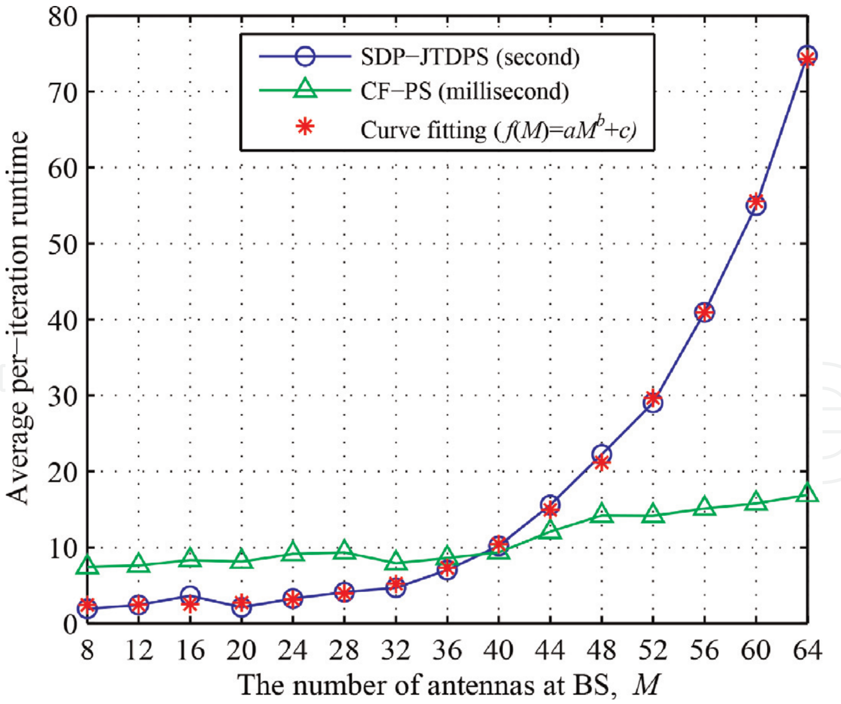

Figure 6.
Comparison of computational complexity.

with equality for both schemes. It is also shown that the SDP-JTDPS can exactly reach the EH targets of all users, which implies that the EH constraints are satisfied with equality. Different from the SDP-JTDPS, the CF-PS harvests more energy than the predefined threshold, but at the expense of more transmit power, which is shown in **Figure 5**.

The optimized transmit power achieved by the algorithms are compared in **Figure 5**. During the simulations, all algorithms run at the same independently generated initial receivers in each trail. It can be observed that SDP-JTDPS and CF-PS consume higher transmit power than the traditional MSE-QoS-TRAD at most of the trials, and CF-PS consumes more power than SDP-JTDPS. This is obvious because more power is needed to satisfy the EH requirements. CF-PS consumes more transmit power than SDP-JTDPS does, which has been mentioned in the previous section that the low complexity is achieved at the cost of high transit power.

As shown in **Figure 6**, CF-PS performs the best with respect to the computational complexity. For the SDP-JTDPS scheme, its execution time is well fitted as a power function on the number of transmit antennas M with $a = 2.662 \times 10^{-7}$, $b = 4.608$, and $c = 2.408$. This is exactly coherent with the complexity analysis in Section 2.3.4.

3. Joint transceiver design and power splitting optimization based on SINR criterion for MIMO IC channel

In this section, we further consider the joint transceiver design and wireless power transfer for MIMO IC networks.

3.1 System model

A K-user MIMO IC network as shown in **Figure 7** is considered. Without loss of generality, a symmetric configuration, that is, each user consists of a pair of

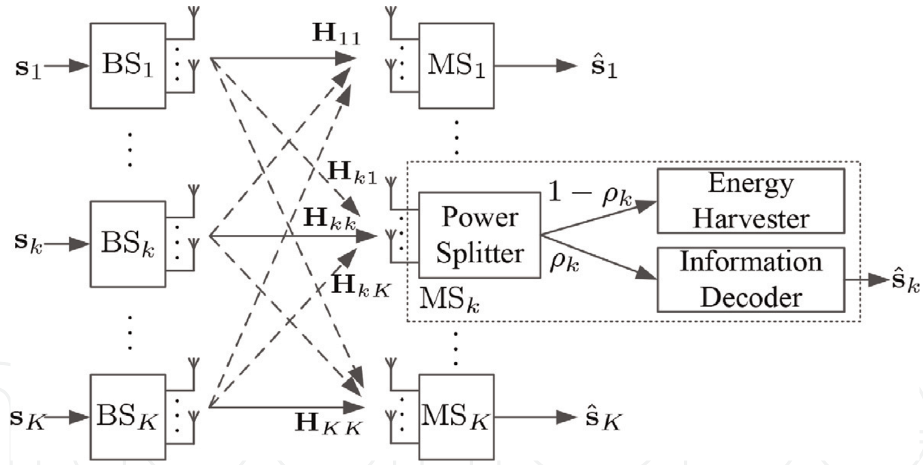

Figure 7.
MIMO interference channel SWIPT system.

transmitters with n_t transmit antennas and nr receive antennas and each user transmits d data streams from its transmitter to its receiver, is assumed. For simplicity, the MIMO IC network is henceforth denoted by $(nt, nr, d)^K$. It is assumed that the transceiver pairs share the same frequency band and operate in SWIPT mode. The channel matrix from transmitter j to receiver k is denoted by $\mathbf{H}_{kj} \in \mathcal{C}^{n_r \times n_t}, \forall k, j \in \{1, \dots, K\}$, in which $\mathbf{H}_{kk}$ describes the channel coefficients of the desired direct link of the kth user pair, and $\mathbf{H}_{kj}, \forall j \neq k$ constitutes channel coefficients of all interference links. It is assumed that $\mathbf{s}_j \in \mathcal{C}^{d \times 1}$ denotes the data vector of the jth transmitter and assumes $\mathbb{E}\left[\mathbf{s}_j \mathbf{s}_j^{\mathrm{H}}\right] = \mathbf{I}_d$. After being precoded by a matrix $\mathbf{V}_k \in \mathcal{C}^{n_t \times d}$, it will be launched over the wireless channel. The transmit power of the kth transmitter can be calculated as $\mathbb{E}\left[\mathrm{Tr}\left(\mathbf{V}_j \mathbf{V}_j^{\mathrm{H}}\right)\right] = P_j$.

The received baseband signal at the kth receiver is written as

$$\mathbf{r}_k = \mathbf{H}_{kk}\mathbf{V}_k\mathbf{s}_k + \sum_{j=1,\, j\neq k}^{K} \mathbf{H}_{kj}\mathbf{V}_j\mathbf{s}_j + \mathbf{n}_k, \tag{33}$$

where $\mathbf{n}_k \in \mathcal{C}^{n_r \times 1}$ is the noise vector at the kth receiver, whose elements are assumed to be i.i.d. complex Gaussian random variables with variance $\sigma^2_{\mathbf{n}_k}$.

Similar to Section 2.1, the received signal at each antenna is then divided into two parts via a power splitter; one part is for information decoding, and the other is transformed to stored energy. The signal split into the ID receiver at the kth user is expressed as

$$\mathbf{r}_k^{ID} = \sqrt{\rho_k}\left(\mathbf{H}_{kk}\mathbf{V}_k\mathbf{s}_k + \sum_{j=1,\, j\neq k}^{K} \mathbf{H}_{kj}\mathbf{V}_j\mathbf{s}_j + \mathbf{n}_k\right) + \mathbf{w}_k, \tag{34}$$

where $\mathbf{w}_k \sim \mathcal{CN}\left(\mathbf{0}, \sigma^2_{\mathbf{w}_k}\mathbf{I}_{n_r}\right)$ is the additive complex Gaussian noise introduced by the power splitter.

Define $\mathbf{U}_k$ to be the receive filter for information decoding at the kth receiver, the detected signal is written as

$$\hat{\mathbf{s}}_k = \sqrt{\rho_k}\mathbf{U}_k^H\mathbf{r}_k^{ID}$$
$$= \underbrace{\sqrt{\rho_k}\mathbf{U}_k^H\mathbf{H}_{kk}\mathbf{V}_k\mathbf{s}_k}_{\text{Desired Signal}} + \underbrace{\sum_{j=1,\, j\neq k}^{K} \sqrt{\rho_k}\mathbf{U}_k^H\mathbf{H}_{kj}\mathbf{V}_j\mathbf{s}_j}_{\text{Interference}} + \underbrace{\sqrt{\rho_k}\mathbf{U}_k^H\mathbf{n}_k + \mathbf{U}_k^H\mathbf{w}_k}_{\text{Noise}}. \tag{35}$$

The SINR of the lth data stream of the kth user is defined as

$$\text{SINR}_{kl} = \frac{\rho_k\left|\mathbf{u}_{kl}^H\mathbf{H}_{kk}\mathbf{v}_{kl}\right|^2}{\sum_{(j,m)\neq(k,l)}\rho_k\left|\mathbf{u}_{kl}^H\mathbf{H}_{kj}\mathbf{v}_{jm}\right|^2 + \left(\rho_k\sigma_n^2 + \sigma_w^2\right)\mathbf{u}_{kl}^H\mathbf{u}_{kl}}, \tag{36}$$

where $\mathbf{u}_{kl}$ and $\mathbf{v}_{kl}$ denote the lth column vector in $\mathbf{U}_k$ and $\mathbf{V}_k$, respectively.

Let $\xi_k \in (0, 1]$ be the energy conversion efficiency, the harvested energy at the kth receiver writes

$$P_k^{\text{EH}} = \xi_k(1-\rho_k)\left[\sum_{j=1}^{K}\text{Tr}\left(\mathbf{H}_{kj}\mathbf{V}_j\mathbf{V}_j^H\mathbf{H}_{kj}^H\right) + n_r\sigma_{\mathbf{n}_k}^2\right]. \tag{37}$$

3.2 Problem formulation

To minimize the transmit power under the given QoS constraints, the joint transceiver design and power splitting problem is formulated as

$$\min_{\{\mathbf{U}_k, \mathbf{V}_k, \rho_k\}} \quad \sum_{k=1}^{K}\sum_{l=1}^{d}\|\mathbf{v}_{kl}\|_2^2 \tag{38}$$
$$s.t.: \quad \text{SINR}_{kl} \geq \gamma_{kl}, \tag{39}$$
$$P_k^{\text{EH}} \geq \psi_k, \tag{40}$$
$$0 \leq \rho_k \leq 1, \forall(k,l). \tag{41}$$

Here, SINR is adopted to measure the QoS of ID. Eqs. (38–41) are nonconvex, and thus, it is very difficult to obtain its optimal solution. Similar to Section 2.1, the AO framework can be adopted to develop an iterative algorithm. In order to achieve this, the concept of interference alignment can be utilized. Therefore, some preliminaries on IA are introduced in the following section.

3.3 Interference alignment

IA is a ground-breaking interference management method for IC networks. The idea of IA is to coordinate the transmitters so that the interference received at each receiver can be aligned into a subspace with a small dimension and thus leaves the interference-free subspace for signal [28]. IA has the ability to achieve the maximum degrees of freedom (DoF) of the K-user IC networks.

As shown in **Figure 1**, when the EH receivers are removed, the system degenerates into traditional symmetric MIMO IC networks. The DoF of such MIMO IC network is $\min(n_t, n_r)K/2$ [28, 29]. To achieve IA, the following feasibility condition should be satisfied [30].

$$\mathbf{U}_k^{\text{H}}\mathbf{H}_{kj}\mathbf{V}_j = \mathbf{0} \ \ , \forall j, k \in \{1, \dots, K\}, j \neq k \tag{42}$$

$$rank\left(\mathbf{U}_k^{\mathrm{H}}\mathbf{H}_{kk}\mathbf{V}_k\right) = d, \tag{43}$$

When the condition (42) is satisfied, the inter-user interference can be completely suppressed. While the condition (43) guarantees that sufficient dimensions are left for signal subspace. For the considered system, in order to achieve IA, the maximum number of streams for each user should no more than $d \le (n_t + n_r)/(K+1)$ [31]. Since the IA condition is over constrained, it is not trivial to develop closed-form solution for it. In literature, a lot of iterative algorithms have been developed, such as the MIL algorithm [30], max-SINR algorithm [30], and MMSE algorithm [32].

If IA conditions are perfectly satisfied, and the received signal of user k reduces to

$$\hat{\mathbf{s}}_k = \mathbf{U}_k^{\mathrm{H}}\mathbf{r}_k = \overline{\mathbf{H}}_k\mathbf{s}_k + \overline{\mathbf{n}}_k, \tag{44}$$

where $\overline{\mathbf{H}}_k = \mathbf{U}_k^{\mathrm{H}}\mathbf{H}_{kk}\mathbf{V}_k$ and $\overline{\mathbf{n}}_k = \mathbf{U}_k^{\mathrm{H}}\mathbf{n}_k$ denote the effective channel matrix and the effective noise vector at receiver k, respectively.

Eq. (44) means that the system is equivalent to a traditional point-to-point MIMO system after IA and the ergodic achievable rate of the kth user is

$$\mathcal{R}_k = \mathbb{E}\left[\log_2\left|\mathbf{I}_d + \frac{\overline{\mathbf{H}}_k\overline{\mathbf{H}}_k^{\mathrm{H}}}{\sigma_{\mathbf{n}_k^2}}\right|\right]. \tag{45}$$

In the following sections, the feasibility of the formulated problem (38) will be discussed, and suboptimal schemes solving the problem will be developed.

3.4 Feasibility analysis

The feasibility of the formulated problems (38–41) can be given by the following propositions [14].

Proposition 7 Problem (38) is feasible if and only if the following problem is feasible.

$$\begin{aligned} \text{Find}: \quad & \{\mathbf{U}_k, \mathbf{V}_k, \rho_k\} \\ \text{Such that}: \quad & \text{SINR}_{kl} \ge \gamma_{kl}, \\ & 0 \le \rho_k \le 1, \forall(k,l). \end{aligned} \tag{46}$$

Proposition 8 Problem (46) is feasible if and only if the following problem is feasible.

$$\begin{aligned} \text{Find}: \quad & \{\mathbf{U}_k, \mathbf{V}_k\} \\ \text{Such that}: \quad & \text{SINR}'_{kl} \ge \gamma_{kl}, \forall(k,l), \end{aligned} \tag{47}$$

where

$$\text{SINR}'_{kl} = \frac{\left|\mathbf{u}_{kl}^H\mathbf{H}_{kk}\mathbf{v}_{kl}\right|^2}{\sum_{(j,m)\ne(k,l)}\left|\mathbf{u}_{kl}^H\mathbf{H}_{kj}\mathbf{v}_{jm}\right|^2 + \left(\sigma_n^2 + \sigma_w^2\right)\mathbf{u}_{kl}^H\mathbf{u}_{kl}}. \tag{48}$$

Proposition 7 and Proposition 8 show that the feasibility of (38–41) is independent of the EH constraints and the PS factors. Proposition 8 is a sufficient and necessary condition for the feasibility of problem (38–41). However, it is not hard to solve (47) [33, 34] directly since SINRs are overconstrained. As an alternative, a sufficient condition for the feasibility of problem (47) is derived based on IA by the following proposition.

Proposition 9 (47) is feasible for any given SINR constraints if the system is interference unlimited, that is, the interference can be completely eliminated by the linear transceivers.

Proof. If interference is completely eliminated, given the transceivers $\mathbf{U}_k, \mathbf{V}_k, \forall k$, that is,

$$\mathbf{u}_{kl}^{\mathrm{H}}\mathbf{H}_{kj}\mathbf{v}_{jm} = \mathbf{0}, \forall (j,m) \neq (k,l), \tag{49}$$

$$\mathbf{u}_{kl}^{\mathrm{H}}\mathbf{H}_{kk}\mathbf{v}_{kl} \neq 0, \forall (k,l), \tag{50}$$

SINR (48) becomes

$$\mathrm{SINR}_{kl}' = \frac{\left|\mathbf{u}_{kl}^{\mathrm{H}}\mathbf{H}_{kk}\mathbf{v}_{kl}\right|^2}{\left(\sigma_n^2 + \sigma_w^2\right)\mathbf{u}_{kl}^H\mathbf{u}_{kl}} = \frac{p_{kl}\left|\mathbf{u}_{kl}^{\mathrm{H}}\mathbf{H}_{kk}\overline{\mathbf{v}}_{kl}\right|^2}{\left(\sigma_n^2 + \sigma_w^2\right)\|\mathbf{u}_{kl}\|_2^2}, \tag{51}$$

where $\overline{\mathbf{v}}_{kl} = \frac{\mathbf{v}_{kl}}{\|\mathbf{v}_{kl}\|_2}$ is the normalized precoding vector, p_{kl} is the transmit power along the beamforming direction $\overline{\mathbf{v}}_{kl}$ and $\mathbf{v}_{kl} = p_{kl}\overline{\mathbf{v}}_{kl}$. According to (51), the SINR constraints in problem (47) can always be satisfied by increasing the transmit power p_{kl}, if the interference is completely suppressed.

Based on Proposition 9 and the IA feasibility condition (35), problems (38–41) must be feasible if the system is IA feasible. In the following, it is assumed that the considered MIMO IC network is IA feasible.

3.5 Alternative optimization solution based on semidefinite programming relaxation

An iterative algorithm for (38–41) can be developed based on AO framework, that is, alternatively optimizing the transmitters $\mathbf{V}_k, \forall k$ together with the PS factors $\rho_k, \forall k$ and the receivers $\mathbf{U}_k, \forall k$.

3.5.1 Transmitter and power splitting optimization

When the receivers are fixed, problems (38–41) are reduced to the following joint transmit precoders and PS factors optimization problem

$$\begin{aligned} &\min_{\{\mathbf{v}_{kl}, \rho_k, \forall (k,l)\}} \quad \sum_{k=1}^{K}\sum_{l=1}^{d} \|\mathbf{v}_{kl}\|_2^2 \\ &\text{s.t.}: \quad \frac{\left|\mathbf{u}_{kl}^H\mathbf{H}_{kk}\mathbf{v}_{kl}\right|^2}{\mathbf{u}_{kl}\mathbf{B}_{kl}\mathbf{u}_{kl}^H} \geq \gamma_{kl}, \\ &\qquad \sum_{j=1}^{K}\sum_{m=1}^{d} \|\mathbf{H}_{kj}\mathbf{v}_{jm}\|_2^2 \geq \frac{\psi_k}{\xi_k(1-\rho_k)} - n_r\sigma_n^2, \\ &\qquad 0 \leq \rho_k \leq 1, \forall (k,l), \end{aligned} \tag{52}$$

where $\mathbf{B}_{kl} = \sum_{j=1}^{K}\sum_{m=1}^{d}\mathbf{H}_{kj}\mathbf{v}_{jm}\mathbf{v}_{jm}^H\mathbf{H}_{kj}^H - \mathbf{H}_{kk}\mathbf{v}_{kl}\mathbf{v}_{kl}^H\mathbf{H}_{kk}^H + \left(\sigma_n^2 + \frac{\sigma_w^2}{\rho_k}\right)\mathbf{I}_{n_r}$.

According to Lemma 8, Proposition 9, and [35], Proposition 9, problem (52) is feasible if the original problem is feasible. By defining $\mathbf{X}_{kl} = \mathbf{v}_{kl}\mathbf{v}_{kl}^H, \mathbf{X}_{kl} \succeq \mathbf{0}$, problem (52) can be relaxed as the following convex SDP program

$$\begin{aligned}
&\min_{\{\mathbf{X}_{kl},\rho_k,\forall(k,l)\}} \quad \sum_{k=1}^{K}\sum_{l=1}^{d}\mathrm{Tr}(\mathbf{X}_{kl}) \\
&\text{s.t.}: \quad (1+\gamma_{kl})\mathrm{Tr}\left(\mathbf{u}_{kl}^{\mathrm{H}}\mathbf{H}_{kk}\mathbf{X}_{kl}\mathbf{H}_{kk}^{H}\mathbf{u}_{kl}\right) \\
&\quad -\gamma_{kl}\sum_{j=1}^{K}\sum_{m=1}^{d}\mathrm{Tr}\left(\tilde{\mathbf{u}}_{kl}^{\mathrm{H}}\mathbf{H}_{kj}\mathbf{X}_{jm}\mathbf{H}_{kj}^{H}\mathbf{u}_{kl}\right) \geq \gamma_{kl}\left(\sigma_n^2+\frac{\sigma_w^2}{\rho_k}\right)\|\mathbf{u}_{kl}\|_2^2, \\
&\quad \sum_{j=1}^{K}\sum_{m=1}^{d}\mathrm{Tr}\left[\mathbf{H}_{kj}\mathbf{X}_{jm}\mathbf{H}_{kj}^{H}\right] \geq \frac{\psi_k}{\xi_k(1-\rho_k)} - n_r\sigma_n^2, \\
&\quad 0 \leq \rho_k \leq 1, \forall(k,l).
\end{aligned} \tag{53}$$

The convex SDP (53) can be solved efficiently. Moreover, it can be proven that there is $rank(\mathbf{X}_{kl}) = 1$ and the SDP relaxation is tight [34], meaning that the optimal solution of the relaxed problem is also optimal to the original problem. After obtaining the rank-one solution $\{\mathbf{X}_{kl}, \forall(k,l)\}$, the optimal solution $\mathbf{v}_{kl}$ to problem (52) can be further recovered from the eigen decomposition of $\mathbf{X}_{kl}$.

3.5.2 Receiver optimization

When the transmit precoders and PS factors are all fixed, (38–41) become separable with respect to variables $\{\mathbf{u}_{kl}, \forall(k,l)\}$. Recall that the SINR constraints have been satisfied by the solution of (52), we can further maximize the receive per-stream SINR by

$$\max_{\mathbf{u}_{kl}} \frac{\mathbf{u}_{kl}^{\mathrm{H}}\mathbf{H}_{kk}\mathbf{v}_{kl}\mathbf{v}_{kl}^{H}\mathbf{H}_{kk}^{H}\mathbf{u}_{kl}}{\mathbf{u}_{kl}^{H}\mathbf{B}_{kl}\mathbf{u}_{kl}} \tag{54}$$

where $\mathbf{B}_{kl} = \sum_{j=1}^{K}\sum_{m=1}^{d}\mathbf{H}_{kj}\mathbf{v}_{jm}\mathbf{v}_{jm}^{\mathrm{H}}\mathbf{H}_{kj}^{\mathrm{H}} - \mathbf{H}_{kk}\mathbf{v}_{kl}\mathbf{v}_{kl}^{\mathrm{H}}\mathbf{H}_{kk}^{\mathrm{H}} + \left(\sigma_n^2 + \frac{\sigma_w^2}{\rho_k}\right)\mathbf{I}_{n_r}$. Eq. (54) is a generalized Rayleigh quotient and its closed-form solution is given by

$$\mathbf{u}_{kl} = \frac{\mathbf{B}_{kl}^{-1}\mathbf{H}_{kk}\mathbf{v}_{kl}}{\|\mathbf{B}_{kl}^{-1}\mathbf{H}_{kk}\mathbf{v}_{kl}\|_2}. \tag{55}$$

3.5.3 Algorithm description

By alternatively optimizing the transmitters together with PS factors and the receivers, an SDP-based joint transceiver design and PS optimization scheme can be obtained, which is summarized in Algorithm 3.

Algorithm 3 Joint transceiver design and power splitting based on SDP (SDP-JTDPS).

1: Initialize the receivers $\mathbf{U}_k, \forall k$.
2: Solve the convex problem (53) to obtain $\mathbf{X}_{kl}$ and power splitting factors $\rho_k, \forall(k,l)$.
3: Recover $\mathbf{v}_{kl}, \forall(k,l)$ from $\mathbf{X}_{kl}$ through eigenvalue decomposition.
4: Update the receiver $\mathbf{u}_{kl}, \forall(k,l)$ by (55).
5: Repeat 2 to 4 until convergence or the maximum iteration number reached.

The convergence of Algorithm 3 is given by the following proposition [14].

Proposition 10 If (53) is feasible for the initial receivers $\mathbf{U}_k, \forall k$, the convergence to a locally optimal solution can be guaranteed by Algorithm 3.

According to Proposition 10, it is important to initialize the receivers $\mathbf{U}_k, \forall k$ for the success of the algorithm. To guarantee finding a feasible solution to (53), we initialize the receivers by the IA receivers $\mathbf{U}_k^{IA}, \forall k$ in this chapter. Similar to Algorithm 1, the complexity of Algorithm 3 is dominated by the SDP solving process, which is about $\mathcal{O}\left((n_r Kd)^{4.5} \log(1/\epsilon)\right)$ for one instance [10]. This complexity becomes prohibitive as the number of antennas or users increases. In the following section, a low-complexity design schemes solving this problem is developed.

3.6 Low-complexity design schemes

Two kinds of low complexity schemes are derived to solve problems (38–41) by separately designing the transceivers and power splitting factors. The transceivers are firstly designed by eigen-decomposing the effective channel matrices generated by interference alignment. Then, the transmit power and receive PS factors are optimized with the precoders and receivers fixed.

As analyzed in the previous section, to ensure that (38–41) are feasible, perfect IA should be realized. To simplify the system design, we assume that the precoders and receive filters are orthogonalized such that $\left(\mathbf{V}_k^{\text{IA}}\right)^{\text{H}}\mathbf{V}_k^{\text{IA}} = \mathbf{I}_d$ and $\left(\mathbf{U}_k^{\text{IA}}\right)^{\text{H}}\mathbf{U}_k^{\text{IA}} = \mathbf{I}_d$. Given interference alignment transceivers, the effective channel matrix for user k can be decomposed as $\overline{\mathbf{H}}_{kk} = \left(\mathbf{U}_k^{\text{IA}}\right)^{\text{H}}\mathbf{H}_{kk}\mathbf{V}_k^{\text{IA}} = \overline{\mathbf{U}}_k\boldsymbol{\Lambda}_k\overline{\mathbf{V}}_k^{\text{H}}$ through singular value decomposition (SVD), where $\boldsymbol{\Lambda}_k = \text{diag}\left(\sqrt{\lambda_{k1}}, \sqrt{\lambda_{k2}}, \dots, \sqrt{\lambda_{kd}}\right)$ is a diagonal matrix. The transmit precoder matrix can be constructed as $\mathbf{V}_k' = \mathbf{V}_k^{\text{IA}}\overline{\mathbf{V}}_k$. By further multiplying the power matrix, the transmit precoding vector is then finally constructed as $\mathbf{V}_k = \mathbf{V}_k'\mathbf{P}_k$, where $\mathbf{P}_k = \text{diag}\left(\sqrt{p_{k1}}, \dots, \sqrt{p_{kd}}\right)$ is a diagonal matrix with nonnegative diagonalized elements. At the receiver side, the receive filter is constructed similarly, $\mathbf{U}_k = \mathbf{U}_k^{\text{IA}}\overline{\mathbf{U}}_k$. Then, the following equations are established

$$\mathbf{U}_k^{\text{H}}\mathbf{H}_{kj}\mathbf{V}_j = \mathbf{0} \ , \forall j, k \in \{1, \dots, K\}, j \neq k, \tag{56}$$

$$\mathbf{U}_k^{\text{H}}\mathbf{H}_{kk}\mathbf{V}_k = \boldsymbol{\Lambda}_k\mathbf{P}_k, \forall k. \tag{57}$$

Eq. (56) shows that interference is completely suppressed at the ID receiver by the transceiver design scheme. According to Lemma 7, Lemma 8, and Proposition 9, we know that problems (38–41) are feasible and can be reduced to the following transmit power allocation and power splitting problem

$$\begin{aligned}
&\min_{\{p_{kl}, \rho_k, \forall k, l\}} \quad \sum_{k=1}^{K}\sum_{l=1}^{d} p_{kl} \\
\text{s.t.}:\quad & \frac{\rho_k \lambda_{kl} p_{kl}}{\left(\rho_k\sigma_n^2 + \sigma_w^2\right)\|\mathbf{u}_{kl}\|_2^2} \geq \gamma_{kl}, \\
& \xi_k(1-\rho_k)\left(\sum_{j=1}^{K}\sum_{m=1}^{d} p_{jm}\|\mathbf{H}_{kj}\mathbf{v}_{jm}'\|_2^2 + n_{\text{r}}\sigma_n^2\right) \geq \psi_k, \\
& 0 \leq \rho_k \leq 1, \forall (k, l).
\end{aligned} \tag{58}$$

In the following, two different schemes solving (58) is developed by either reformulating it as a convex problem or solved in closed form.

3.6.1 Optimal power allocation and power splitting scheme

After some algebraic manipulations, problem (58) can be reformed as

$$\begin{aligned} \min_{\{p_{kl},\rho_k,\forall k,l\}} \quad & \sum_{k=1}^{K}\sum_{l=1}^{d} p_{kl} \\ \text{s.t.}: \quad & p_{kl} - \frac{\sigma_n^2\gamma_{kl}\|\mathbf{u}_{kl}\|_2^2}{\lambda_{kl}} \geq \frac{\sigma_w^2\|\mathbf{u}_{kl}\|_2^2\gamma_{kl}}{\lambda_{kl}\rho_k}, \\ & \sum_{j=1}^{K}\sum_{m=1}^{d} p_{jm}\|\mathbf{H}_{kj}\mathbf{v}'_{jm}\|_2^2 \geq \frac{\psi_k}{\xi_k(1-\rho_k)} - n_r\sigma_n^2, \\ & 0 \leq \rho_k \leq 1, \forall(k,l). \end{aligned} \tag{59}$$

Problem (59) is convex and thus can be solved optimally. Denote p_{kl}^* and ρ_k^*, $\forall k$ as its optimal solution, the transmit precoders are $\mathbf{v}_{kl} = \sqrt{p_{kl}^*}\mathbf{v}_{kl}^{\mathrm{IA}}$.

The proposed IA-based SWIPT scheme with optimal power allocation and power splitting is summarized in Algorithm 4. The computational complexity of Algorithm 4 is mainly from solving (59) in Step 4. When the interior methods are employed, the computational complexity of Algorithm 4 is in the order of $\mathcal{O}\left((Kd)^3\right)$ [27], which is significantly lower than that of Algorithm 3.

Algorithm 4 SWIPT design with optimal transmit power allocation and receive power splitting over effective IA channel decomposing (O-PAPS).

1: Obtain IA transceivers $\{\mathbf{U}_k^{\mathrm{IA}}, \mathbf{V}_k^{\mathrm{IA}},\ \forall k\}$ that satisfy the IA conditions.
2: Let $\overline{\mathbf{H}}_{kk} = \left(\mathbf{U}_k^{\mathrm{IA}}\right)^{\mathrm{H}}\mathbf{H}_{kk}\mathbf{V}_k^{\mathrm{IA}}, \forall k$, and decompose $\overline{\mathbf{H}}_{kk}$ as $\overline{\mathbf{H}}_{kk} = \overline{\mathbf{U}}_k \mathbb{L}_k \overline{\mathbf{V}}_k^{\mathrm{H}}$ through SVD, where $\boldsymbol{\Lambda}_k = \mathrm{diag}\left(\sqrt{\lambda_{k1}}, \sqrt{\lambda_{k2}}, \dots, \sqrt{\lambda_{kd}}\right)$.
3: Let $\mathbf{U}_k = \mathbf{U}_k^{\mathrm{IA}}\overline{\mathbf{U}}_k$ and $\mathbf{V}'_k = \mathbf{V}_k^{\mathrm{IA}}\overline{\mathbf{V}}_k, \forall k$.
4: Obtain the optimal transmit power p_{kl}^* and power splitting factors ρ_k^*, $\forall k, l$ by solving the convex problem (59).
5: Set $\mathbf{v}_{kl} = \sqrt{p_{kl}^*}\mathbf{v}_{kl}^{\mathrm{IA}}, \forall k, l$.

3.6.2 Closed-form power allocation and power splitting scheme

Given the IA solution $\{\mathbf{U}_k^{\mathrm{IA}}, \mathbf{V}_k^{\mathrm{IA}}, \forall k\}$, by discarding the EH constraints of (58), we consider the following SINR constrained power optimization problem

$$\begin{aligned} \min_{\{p_{kl},\forall k,l\}} \quad & \sum_{k=1}^{K}\sum_{l=1}^{d} p_{kl} \\ \text{s.t.}: \quad & \frac{\lambda_{kl}p_{kl}}{\left(\sigma_n^2+\sigma_w^2\right)\|\mathbf{u}_{kl}\|_2^2} \geq \gamma_{kl}, \forall(k,l). \end{aligned} \tag{60}$$

According to Proposition 9, (60) is feasible. By further applying Lemma 8, (58) is feasible. Moreover, (60) can be decomposed into $\sum_{k=1}^{K} d$ parallel subproblems. For the l-th data stream of the kth user, the subproblem is expressed as

$$\begin{aligned} \min_{p_{kl}} \quad & p_{kl} \\ \text{s.t.}: \quad & \frac{\lambda_{kl}p_{kl}}{\left(\sigma_n^2+\sigma_w^2\right)\|\mathbf{u}_{kl}\|_2^2} \geq \gamma_{kl}. \end{aligned} \tag{61}$$

The solution of (61) is then given by

$$\hat{p}_{kl} = \frac{\left(\sigma_n^2 + \sigma_w^2\right)\|\mathbf{u}_{kl}\|_2^2\gamma_{kl}}{\lambda_{kl}}. \tag{62}$$

Following Lemma 7, (58) can be optimized by substituting p_{kl} with $\alpha\hat{p}_{kl}$, where $\alpha \geq 1$ is a scaling factor to be optimized. Then, (58) is reduced to a problem jointly optimizing α and PS factors ρ_k under SINR and EH constraints, which is

$$\begin{aligned} &\min_{\alpha,\{\rho_k,\forall k,l\}} \quad \sum_{k=1}^{K}\sum_{l=1}^{d}\alpha\hat{p}_{kl} \\ &\text{s.t.}: \quad \rho_k \geq \frac{\sigma_w^2\|\mathbf{u}_{kl}\|_2^2\gamma_{kl}}{\alpha\lambda_{kl}\hat{p}_{kl} - \sigma_n^2\gamma_{kl}\|\mathbf{u}_{kl}\|_2^2}, \\ &1-\rho_k \geq \frac{\psi_k}{\xi_k\left(\sum_{j=1}^{K}\sum_{m=1}^{d}\alpha\hat{p}_{jm}\|\mathbf{H}_{kj}\mathbf{v}'_{jm}\|_2^2 + n_{\mathrm{r}}\sigma_n^2\right)}, \\ &0 \leq \rho_k \leq 1, \forall (k,l), \\ &\alpha > 1. \end{aligned} \tag{63}$$

The closed-form solution of (63) can be derived and given by the following proposition [14].

Proposition 11 Given the IA transceivers $\left\{\mathbf{U}_k^{\mathrm{IA}}, \mathbf{V}_k^{\mathrm{IA}}, \forall k\right\}$, define $a_{kl} = \sigma_w^2\|\mathbf{u}_{kl}\|_2^2\gamma_{kl}$, $b_{kl} = \sigma_n^2\gamma_{kl}\|\mathbf{u}_{kl}\|_2^2$, $c_{kl} = \lambda_{kl}\hat{p}_{kl}$, $f_k = \xi_k\sum_{j=1}^{K}\sum_{m=1}^{d}\hat{p}_{jm}\xi_k\|\mathbf{H}_{kj}\mathbf{v}'_{jm}\|_2^2$, and $g_k = \xi_k n_{\mathrm{r}}\sigma_n^2$. The optimal solution to (63) is given by

$$\alpha^* = \max_{\forall(k,l)} \alpha_{kl}^*, \tag{64}$$

$$\rho_k^* = \max_{\forall l} \rho_{kl}, \tag{65}$$

where α_{kl}^* is the solution to the equation $\frac{a_{kl}}{\alpha c_{kl} - b_{kl}} + \frac{\psi_k}{\alpha f_k + g_k} = 1 \ (\alpha > 1)$, $\rho_{kl} = \frac{a_{kl}}{\alpha^* c_{kl} - b_{kl}}$.

Given α^* and $\hat{p}_{kl}$, the transmit precoders are then determined by $\mathbf{v}_{kl} = \sqrt{\alpha^*\hat{p}_{kl}}\mathbf{v}'_{kl}$. The proposed IA-based SWIPT scheme with the closed-form transmit power allocation and receive power splitting is summarized in Algorithm 5.

Algorithm 5 SWIPT design with closed-form transmits power allocation and receive power splitting solutions over the effective IA channel decomposing (CF-PAPS).

1: Obtain IA transceivers $\left\{\mathbf{U}_k^{\mathrm{IA}}, \mathbf{V}_k^{\mathrm{IA}},\ \forall k\right\}$ that satisfy the IA conditions.
2: Let $\overline{\mathbf{H}}_{kk} = \left(\mathbf{U}_k^{\mathrm{IA}}\right)^{\mathrm{H}}\mathbf{H}_{kk}\mathbf{V}_k^{\mathrm{IA}}, \forall k$, and decompose $\overline{\mathbf{H}}_{kk}$ as $\overline{\mathbf{H}}_{kk} = \overline{\mathbf{U}}_k\mathbf{\Lambda}_k\overline{\mathbf{V}}_k^{\mathrm{H}}$ through SVD, where $\mathbf{\Lambda}_k = \mathrm{diag}\left(\sqrt{\lambda_{k1}}, \sqrt{\lambda_{k2}}, \dots, \sqrt{\lambda_{kd}}\right)$.
3: Let $\mathbf{U}_k = \mathbf{U}_k^{\mathrm{IA}}\overline{\mathbf{U}}_k$ and $\mathbf{V}'_k = \mathbf{V}_k^{\mathrm{IA}}\overline{\mathbf{V}}_k, \forall k$.
4: Calculate $\hat{p}_{kl} = \frac{\left(\sigma_n^2+\sigma_w^2\right)\|\mathbf{u}_{kl}\|_2^2\gamma_{kl}}{\lambda_{kl}}, \forall (k,l)$.
5: Obtain α^* and $\rho_k^*, \forall k$ according to (64).
6: Set $\mathbf{v}_{kl} = \sqrt{\alpha^*\hat{p}_{kl}}\mathbf{v}_{kl}^{\mathrm{IA}}, \forall (k,l)$.

The computational complexity of Algorithm 5 is determined by the IA transceiver design process in Step 1. For the famous closed-from IA algorithm, the complexity is $\mathcal{O}(n_t^3)$. When the max-SINR or MIL algorithm [30] is applied, the complexity is about $\mathcal{O}\left(n_{iter} \max(n_t, n_r)^3\right)$. No matter which method is adopted, the complexity of Algorithm 5 is much lower than that of Algorithm 3 and Algorithm 4.

3.7 Simulation results and analysis

Simulations are done over the wireless system as described in Section 3.1, by setting the number of users $K = 3$ or $K = 4$. The entries of $\mathbf{H}_{kj}$ are assumed to be i.i.d. zero mean complex Gaussian random variables with variance $r_{kj}^{-\beta}$, where r_{kj} is the distance in meters between the jth transmitter and the kth receiver, and β is the path loss factor. The parameters of the symmetric network are set to be $n_t = n_r$, $r_{kl} = r = 5$, $\beta = 2.7$, $\sigma_n^2 = -70$ dBm, $\sigma_w^2 = -50$ dBm, $\xi_{kl} = \xi = 0.8$, $\gamma_{kl} = \gamma$, and $\psi_k = \psi$. For the three-user network, the closed-form MIMO linear IA algorithm given in [28] is adopted to design IA transceivers. For the four-user network, the MIL algorithm [30] is used. The simulation results are obtained by taking the average of the simulation results of all 100 channel realizations.

Figure 8 shows the convergence performance of SDP-JTDPS with $\gamma = \{0, 20\}$ dB and $\psi = \{0, 10\}$ dBm for one channel realization of the $(4, 4, 2)^3$ network. It can be observed that the algorithm converges monotonically, which verifies the convergence analysis.

The empirical cumulative distribution function (CDF) of the output per-stream SINR for the $(4, 4, 2)^3$ network is shown in **Figure 9**. The SINR target γ is 20 dB, and the EH target is 0 and 30 dBm, respectively. The results show that the achieved SINR values exceed the given 20 dB, meaning that the proposed schemes can satisfy the SINR constraints. The difference is that the achieved SINR value can be greater than the target SINR value for SDP-JTDPS and O-PAPS, while for CF-PAPS, the achieved SINR values are always equal to the SINR target, which implies that the EH constraints are satisfied with equality in CF-PAPS.

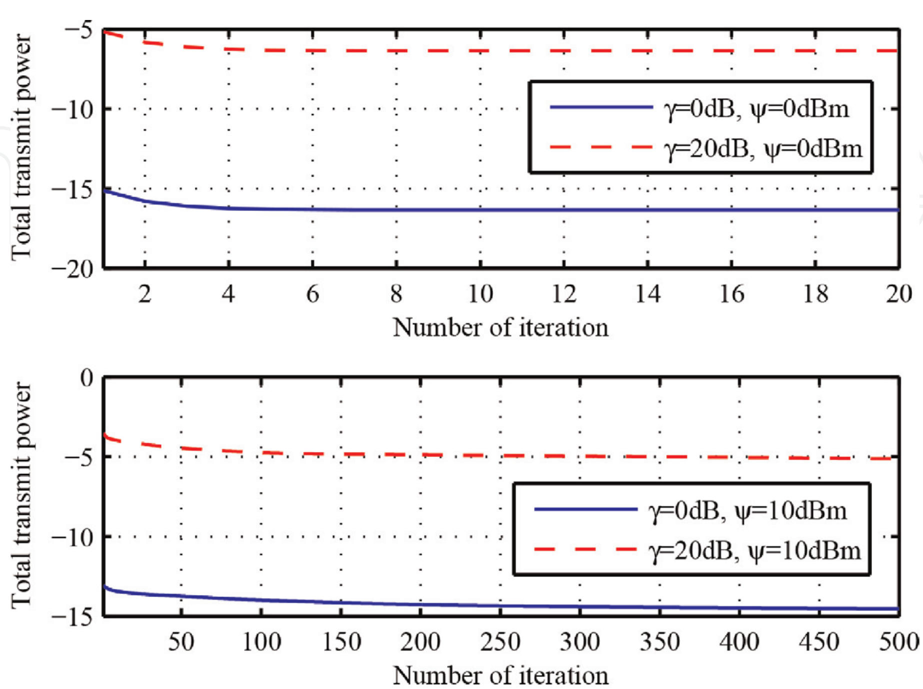

Figure 8.
Convergence property of the semidefinite programming (SDP)-joint transceiver design and power splitting (JTDPS) scheme for the $(4, 4, 2)^3$ network.

Figure 10 shows the total transmit power versus SINR thresholds at different EH thresholds. It is observed that the transmit power will increase along with the increasing of the EH threshold from −10 to 30 dBm when the SINR threshold is fixed. This is because more transmit power is needed to support higher EH requirements. When the SINR threshold is low, the SDP-JTDPS performs the best, and the O-PAPS schemes achieve almost the same performance, and both of them outperform the CF-PAPS scheme. However, when the SINR threshold is high, the SDP-JTDPS scheme performs worse than the O-PAPS scheme and even worse than the CF-PAPS scheme. From the derivation of the algorithms, we expect that the SDP-JTDPS achieves the best performance, but it does not at high SINR regime. The reason is that when SINR is high, the convergence becomes slow, but we set the fixed iteration number in our simulations. Moreover, the difference between the CF-PAPS and O-PAPS will tend to zero as the SINR threshold becomes high. This

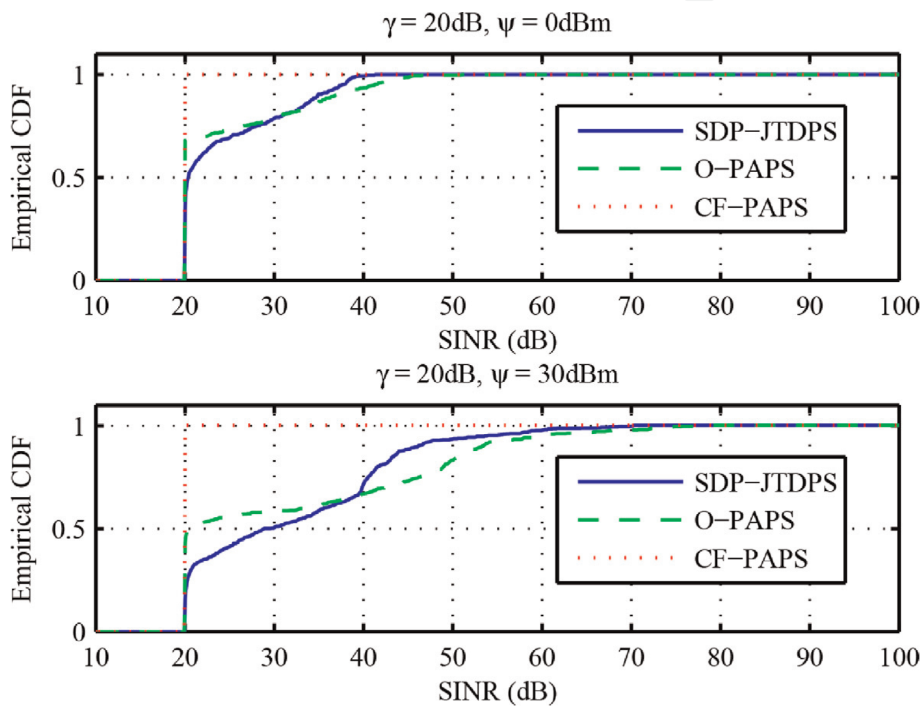

Figure 9.
Empirical distribution of achieved SINR at ID receivers with different SINR and energy harvesting (EH) thresholds for the $(4, 4, 2)^3$.

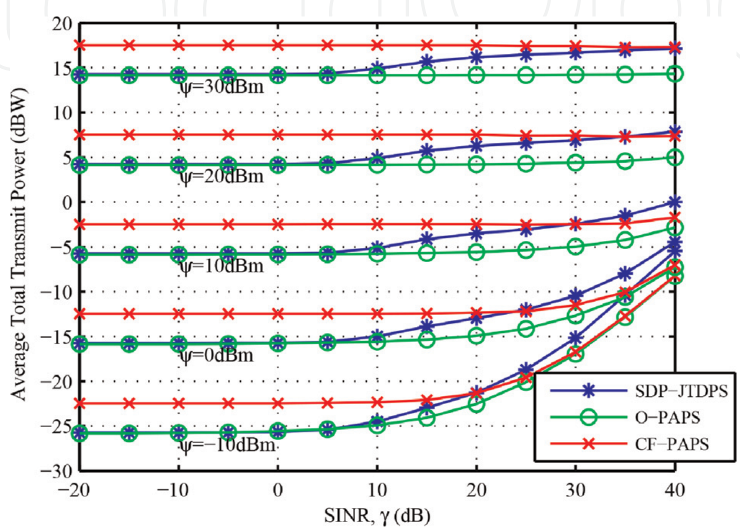

Figure 10.
Average total transmit power versus SINR thresholds for the $(4, 4, 2)^3$.

implies that the performance of the CF-PAPS scheme is asymptotically the same as that of the O-PAPS scheme. The reason can be explained. Specifically, high SINR means high transmit power, and it is well known that the margin reward of the power allocation will tend to zero when the transmit power becomes high.

Figure 11 shows the relationships between the average transmit power and EH thresholds given different SINR targets. It is seen that the average transmit powers asymptotically tend to be the same as the EH threshold increases for any given SINR value for both O-PAPS and CF-PAPS. For any of the three schemes, higher EH requirement means higher transmit power needed. It is also shown that SDP-JTDPS and O-PAPS achieve the same performance when the SINR threshold is relatively low (e.g., $\gamma = -20$ dB). But when the SINR threshold becomes high, SDP-JTDPS performs inferior to the other two schemes significantly at a low EH threshold. The reason is that the convergence speed of SDP-JTDPS tends to slow at that regime. In addition, the performance curves of SDP-JTDPS and CF-PAPS tend to almost the

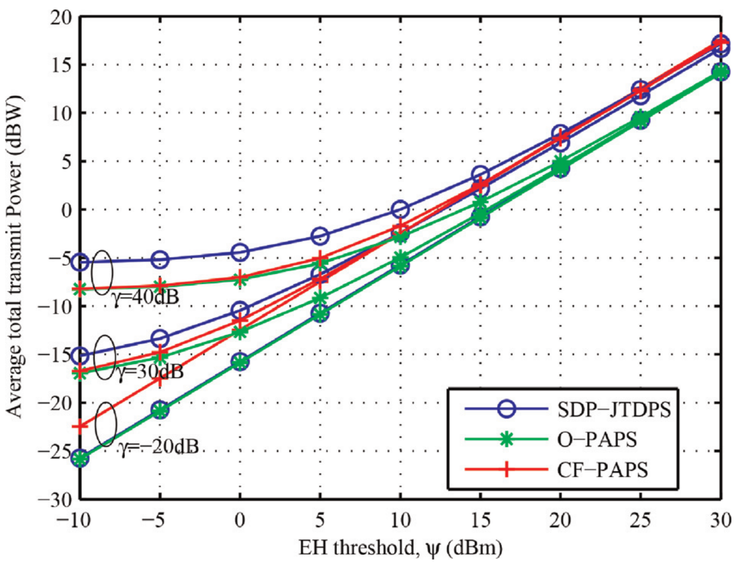

Figure 11.
Average total transmit power versus EH thresholds for the $(4, 4, 2)^3$ *network.*

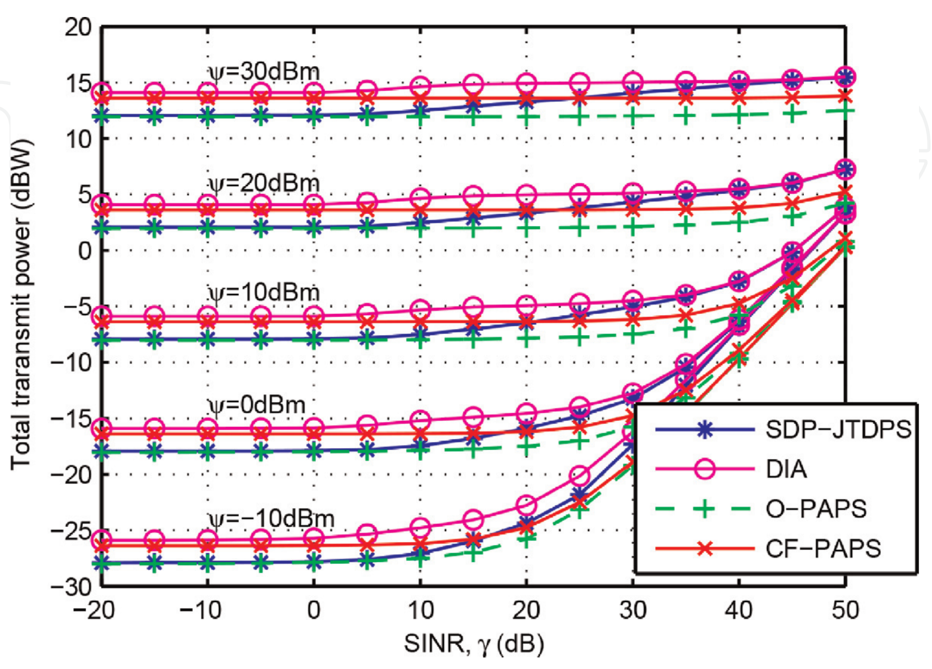

Figure 12.
Total transmit power versus SINR thresholds for the $(6, 6, 2)^4$ *network over one channel realization.*

same when an extremely high EH threshold and a high SINR threshold (e.g., $EH =$ 30 dBm and $\gamma = 40$ dB) are given.

Figure 12 compares SDP-JTDPS with DIA proposed [34] in a $(6, 6, 2)^4$ network over different EH thresholds at fixed SINR values. Note that restricted by its design mechanism, only one data stream is transmitted in the DIA algorithm in the simulation. It can be seen that SDP-JTDPS performs the best, and O-PAPS performs almost the same for low SINR threshold. But when the SINR threshold becomes high, SDP-JTDPS performs worse. This phenomenon is again because SDP-JTDPS has a slower convergence speed when the SINR is high, while the maximum iteration number is set to be 10 in the simulation for saving calculation time. The DIA scheme consumes more transmit power at any given SINR and EH threshold. This is

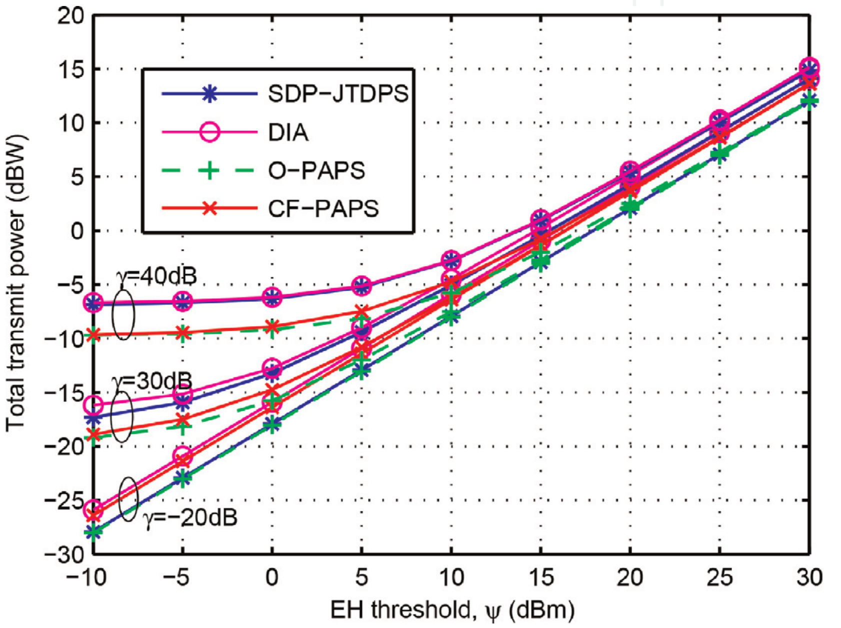

Figure 13.
Total transmit power versus EH thresholds for the $(6, 6, 2)^4$ network over one channel realizations.

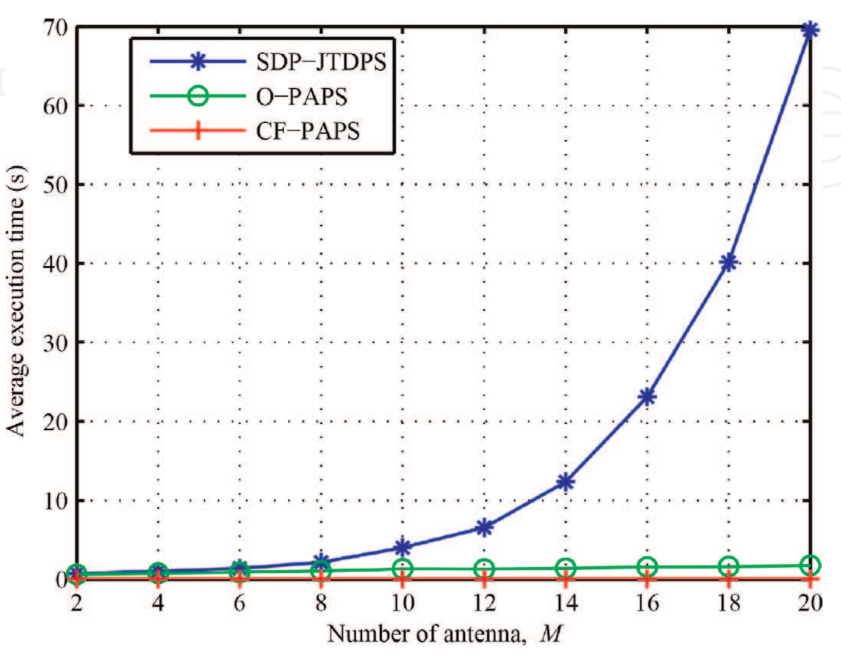

Figure 14.
Average execution time versus M at $\gamma = 10$ dB and $\psi = 10$ dBm.

because only one beamforming vector is utilized at each transmitter in the DIA scheme. Multiplexing gain of SDP-JTDPS helps achieve better performance in transmit power than DIA.

The performance of the proposed schemes is further tested in a $(6, 6, 2)^4$ network. The average transmit powers versus the EH thresholds over different SINR requirements are shown in **Figure 13**. Similar to **Figure 11**, the curves of O-PAPS and CF-PAPS asymptotically tend to be the same for a high EH threshold over all the given SINR thresholds. The curves of DIA also asymptotically tend to be the same over all the given SINR thresholds. The phenomenon reflects that CF-PAPS achieves similar performance with O-PAPS. This is somewhat like the water-filling for the power allocation in traditional MIMO systems where the average power allocation is near optimal at high SNR regimes [36]. Nevertheless, the curves of SDP-JTPDS do not tend to be the same over the observed EH scope. This is because again the convergence speed of SDP-JTPDS will slow down when SINR becomes high. Considering its high computational complexity, the iteration number is set to be 10 in all the simulations.

Finally, **Figure 14** compares the computational complexity of the proposed schemes for different antenna numbers by assuming there are $K = 3$ users. It can be observed that the computational complexity of SDP-JTDPS increases nonlinearly with M, while those of O-PAPS and CF-PAPS increase linearly. Therefore, CF-PAPS and O-PAPS are of much lower complexity than the SDP-based scheme and thus are more attractive for practical applications.

4. Conclusions

The joint transceiver design and power splitting optimization for the simultaneous wireless information and power transfer of the MIMO BC network and IC network are analyzed in this chapter. For the MIMO BC network, a transmit power minimization problem subject to both the EH and MSE constraints is formulated. While for the MIMO IC network, similar transmit power minimization problem is formulated but with the SINR QoS requirements for the ID receivers. Sufficient condition to guarantee the feasibility of nonconvex problems is derived, which reveal that the feasibility of the design problems is not dependent on the PS factors and the EH constraints. Based on the SDP relaxation, alternative solving algorithms are introduced by iteratively optimizing the transmitter together with the PS factors and the receiver. To avoid the high computational complexity of SDP-based schemes, low-complexity algorithms are developed and analyzed. Simulation results have shown the effectiveness of the proposed designs in achieving simultaneous wireless information and power transfer.

Acknowledgements

This work is supported in part by the National Natural Science Foundation of China (NSFC) under grants 61701269 and 61671278, the National Science Fund of China for Excellent Young Scholars under grant 61622111, the Natural Science Foundation of Shandong Province under grant ZR2017BF012, and the Joint Research Foundation for Young Scholars in the Qilu University of Technology (Shandong Academy of Sciences) under grant 2017BSHZ005.

Author details

Anming Dong[1,2,3] and Haixia Zhang[1*]

1 Shandong Provincial Key Laboratory of Wireless Communication Technologies and School of Control Science of Engineering, Shandong University, Jinan, China

2 School of Computer Science and Technology, Qilu University of Technology (Shandong Academy of Sciences), Jinan, China

3 Computer Science Center (National Supercomputer Center in Jinan), Shandong Provincial Key Laboratory of Computer Networks, Qilu University of Technology (Shandong Academy of Sciences), Jinan, China

*Address all correspondence to: haixia.zhang@sdu.edu.cn

References

[1] Bi S, Ho C, Zhang R. Wireless powered communication: Opportunities and challenges. IEEE Communications Magazine. 2015;**53**(4):117-125

[2] Xiao L, Wang P, Niyato D, In Kim D, Han Z. Wireless networks with RF energy harvesting: A contemporary survey. IEEE Communications Surveys and Tutorials. 2014;**17**(2):757-789

[3] Yang H, Clerckx B. Waveform design for wireless power transfer with limited feedback. IEEE Transactions on Wireless Communications. 2017;**17**(1): 415-429

[4] Rezaei O, Naghsh MM, Rezaei Z, Zhang R. Throughput optimization for wireless powered interference channels. IEEE Transactions on Wireless Communications. 2019;**18**(5):2464-2476

[5] Huang K, Zhou X. Cutting the last wires for mobile communications by microwave power transfer. IEEE Communications Magazine. 2015;**53**(6): 86-93

[6] Ho CK, Zhang R. Optimal energy allocation for wireless communications with energy harvesting constraints. IEEE Transactions on Signal Processing. 2012;**60**(9):4808-4818

[7] Gong J, Zhou S, Niu Z. Optimal power allocation for energy harvesting and power grid coexisting wireless communication systems. IEEE Transactions on Communications. 2013; **61**(7):3040-3049

[8] Kang X, Chia Y-K, Ho CK, Sun S. Cost minimization for fading channels with energy harvesting and conventional energy. IEEE Transactions on Wireless Communications. 2014; **13**(8):4586-4598

[9] Zhou S, Chen T, Chen W, Niu Z. Outage minimization for a fading wireless link with energy harvesting transmitter and receiver. IEEE Journal on Selected Areas in Communications. 2015;**33**(3):496-511

[10] Luo Z-Q, Ma W-K, So AM-C, Ye Y, Zhang S. Semidefinite relaxation of quadratic optimization problems. IEEE Signal Processing Magazine. 2010;**27**(3): 20-34

[11] Zhang R, Ho CK. MIMO broadcasting for simultaneous wireless information and power transfer. IEEE Transactions on Wireless Communications. 2013;**12**(5):1989-2001

[12] Zhang H, Dong A, Jin S, Yuan D. Joint transceiver and power splitting optimization for multiuser MIMO SWIPT under MSE QoS constraints. IEEE Transactions on Vehicular Technology. 2017;**66**(8):7123-7135

[13] Dong A, Zhang H, Wu D, Yuan D. QoS-constrained transceiver design and power splitting for downlink multiuser MIMO SWIPT systems. In: IEEE International Conference on Communications (ICC). 2016. pp. 1-6

[14] Dong A, Zhang H, Shu M, Yuan D. Simultaneous wireless information and power transfer for MIMO interference channel networks based on interference alignment. Entropy. 2017; **19**(9):484

[15] Shi Q, Liu L, Xu W, Zhang R. Joint transmit beamforming and receive power splitting for MISO SWIPT systems. IEEE Transactions on Wireless Communications. 2014;**13**(6):3269-3280

[16] Shi Q, Xu W, Chang T-H, Wang Y, Song E. Joint beamforming and power splitting for MISO interference channel with SWIPT: An SOCP relaxation and decentralized algorithm. IEEE Transactions on Signal Processing. 2014; **62**(23):6194-6208

[17] Shi S, Schubert M, Boche H. Downlink MMSE transceiver optimization for multiuser MIMO systems: MMSE balancing. IEEE Transactions on Signal Processing. 2008;**56**(8):3702-3712

[18] Mezghani A, Joham M, Hunger R, Utschick W. Transceiver design for multi-user MIMO systems. Proceedings 10th International ITG/IEEE Workshop on Smart Antennas (WSA). 2006. pp. 1-8

[19] Vucic N, Boche H, Shi S. Robust transceiver optimization in downlink multiuser MIMO systems. IEEE Transactions on Signal Processing. 2009;**57**(9):3576-3587

[20] Beck A. Quadratic matrix programming. SIAM Journal on Optimization. 2007;**17**(4):1224-1238

[21] Ding Y, Ge D, Wolkowicz H. On equivalence of semidefinite relaxations for quadratic matrix programming. Mathematics of Operations Research. 2011;**36**(1):88-104

[22] Huang Y, Palomar DP. Randomized algorithms for optimal solutions of double-sided QCQP with applications in signal processing. IEEE Transactions on Signal Processing. 2014;**62**(5): 1093-1108

[23] Zhu Y, Zhou J, Shen X, Song E, Luo Y. Networked Multisensor Decision and Estimation Fusion*:* Based on Advanced Mathematical Methods. Boca Raton, Florida: CRC Press; 2012

[24] Wang R, Tao M, Huang Y. Linear precoding designs for amplify-and-forward multiuser two-way relay systems. IEEE Transactions on Wireless Communications. 2012;**11**(12): 4457-4469

[25] Vandenberghe L, Boyd S. Semidefinite programming. SIAM Review. 1996;**38**(1):49-95

[26] Michael Grant and Stephen Boyd. 2014CVX: Matlab Software for Disciplined Convex Programming, Version 2.1. Available from: http://cvxr.com/cvx

[27] Boyd S, Vandenberghe L. *Convex Optimization*. Cambridge: Cambridge University Press; 2004

[28] Cadambe VR, Jafar SA. Interference alignment and degrees of freedom of the K-user interference channel. IEEE Transactions on Information Theory. 2008;**54**(8):3425-3441

[29] Gomadam KS, Cadambe VR, Jafar SA. Reflections on interference alignment and the degrees of freedom of the K user interference channel. IEEE Information Theory Society Newsletter. 2009;**59**(4):5-9

[30] Gomadam KS, Cadambe VR, Jafar SA. A distributed numerical approach to interference alignment and applications to wireless interference networks. IEEE Transactions on Information Theory. 2011;**57**(6): 3309-3322

[31] Yetis CM, Gou T, Jafar SA, Kayran AH. On feasibility of interference alignment in MIMO interference networks. IEEE Transactions on Signal Processing. 2010; **58**(9):4771-4782

[32] Shen H, Li B, Tao M, Wang X. MSE-based transceiver designs for the MIMO interference channel. IEEE Transactions on Wireless Communications. 2010; **9**(11):3480-3489

[33] Chiu E, Lau VKN, Huang H, Tao W, Liu S. Robust transceiver design for K-pairs quasi-static mimo interference channels via semi-definite relaxation. IEEE Transactions on Wireless Communications. 2010;**9**(12):3762-3769

[34] Zong Z, Feng H, Richard Yu F, Zhao N, Yang T, Hu B. Optimal

transceiver design for SWIPT in k-user MIMO interference channels. IEEE Transactions on Wireless Communications. 2016;**15**(1):430-445

[35] Wiesel A, Eldar YC, Shamai S. Linear precoding via conic optimization for fixed mimo receivers. IEEE Transactions on Signal Processing. January 2006;**54**(1):161-176

[36] Tse D, Viswanath P. Fundamentals of Wireless Communication. Cambridge: Cambridge University Press; 2005